COMPARISON OF CARBON STEEL AND COMPOSITE SIDE WALL OF LIGHT RAIL VEHICLE BY FINITE ELEMENT ANALYSIS

by

DILRAJ SINGH

THESIS

Submitted in partial fulfillment of the requirements

for the degree of Master of Science in Mechanical Engineering at

The University of Texas at Arlington

May 2017

Acknowledgments

- I would like to express my gratitude towards Dr. Andrey Beyle for his inspiring guidance, encouragement and for investing his valuable time in mentoring me. He always had time to discuss my research work. I have learned to solve problems from the different point of view by his guidance.
- I would like to thank the committee members Dr. Kent L Lawrence and Dr. Wen Shen for agreeing to serve on my thesis defense committee by giving their valuable time and opinions.
- I would like also to like to thank my friends Vedant, Rahul, Anubhav, Nishant and Gurwinder who help me along the way.
- Lastly, I'd like to thank my father, Bahadur Singh, my mother, Manjit Kaur and my younger sister, Priya Raj Kaur for showering their unconditional love and support.

April 26, 2018

Abstract

COMPARISON OF CARBON STEEL AND COMPOSITE SIDE WALL OF

LIGHT RAIL VEHICLE BY FINITE ELEMENT ANALYSIS

DILRAJ SINGH, MS

The University of Texas at Arlington, 2018

Supervising Professor: ANDREY BEYLE

A Railroad car is a vehicle used for carrying passengers and cargo. In the modern era, rail vehicles are designed as lightweight structures with the aim to minimize mass, operational energy demands, and CO_2 emissions. Light rail vehicle is used at street level where they have direct contact with normal traffic and have a short distance between stations. In order to reduce dwell time at stops, and so, the vehicle can accelerate and deaccelerate easily, weight should be less and that is why low floor design is adopted these days. The sidewall is a crucial part of the car body because it stands the weight of the roof, AC unit and ensures the safety of occupants. This thesis research deals with two loads on the side wall of railroad car i.e. Dead load of the roof and the wind load. Lowering the energy usage in railroad rolling stock often requires new weight-out strategies. So, the main motivation is to replace the heavy material carbon steel with advanced composite which can significantly cut weight while establishing great stiffness and strength and delivering vital benefits like reducing the complexity of structure. The main aim of the work is to compare and correlate results obtained from the analysis of various types of materials currently used for Railroad Car body production. Composite Material is recommended for the safe operation of Sidewall panels under dead load of the roof and side wind load replacing the conventional material without compromising the safety. ABAQUS is used for the simulation needs. Effect of above-applied loads on different combination of materials for the side wall structure is studied in addition to modal (Vibration) analysis.

Table of Contents

Acknowledgments……iii

Abstract……iv

List of Illustrations……vii

List of Tables……ix

Chapter 1 Introduction……1

Chapter 2 Motivation and Objective……3

Chapter 3 Literature……4

3.1 History……4

3.2 Sandwich Structures……4

3.3 Function of sandwich structures……5

3.4 Application of Honeycomb Panels……5

3.5 Composite……6

3.6 Classification of composite……7

3.7 The Korean Tilting Train eXpress (TTX)……8

3.8 C20 FICAS……9

3.9 Different types of body shell……9

3.9.1 Fabricated Body Shell……9

3.9.2 Panel Construction Body Shell……9

3.9.3 Hybrid Body Shell……9

Chapter 4 Geometry……10

Chapter 5 Materials……12

5.1 Mild steel……12

5.2 E-glass……12

5.3 Carbon……12

5.4 Epoxy resin……13

5.5 Constraints vs Connectors……15

Chapter 6 Loading & Boundary Conditions……16

6.1 Buckling……16
6.1.1 Analytic Solution……16
6.1.2 Ply sequence……17
6.1.3 Boundary conditions……17
6.2 Wind load……19
6.2.1 Analytic solutions……20
6.2.2 Boundary conditions……20
6.3 Simulation……21
6.4 Constraints……22
6.5 Meshing……23
6.5.1 Buckling Analysis……23
6.5.2 Wind Load……25
6.6 Failure criteria……25
Chapter 7 Results……26
7.1 Buckling Analysis……26
7.1.1 Post Buckling……28
7.1.2 F.O.S vs Displacement……29
7.1.3 Dimension change……30
7.1.4 Sequence change……30
7.1.5 Fasteners change……31
7.1.6 Mass of side wall……32
7.2 Wind Load……33
7.2.1 Sequence change……35
7.3 Natural Frequency……38
7.3.1 Sequence change……39
Chapter 8 Conclusion……41
Chapter 9 Future Work……42
Appendix A Matlab Code……43

Appendix B Mesh Convergence……45

References……46

Biographical Information……48

List of illustrations

Figure 1-1 – 1-3 Car carriage……1

Figure 3-1 Timeline of the body shell evolution……4

Figure 3-2 Sandwich structures……..4

Figure 3-3 Sandwich structure strength……5

Figure 3-4 Use of Honeycomb panels in different industries……6

Figure 3-5 Fiber and Matrix material……..6

Figure 3-6 Classification of composite……7

Figure 3-7 Korean Tilting Train body structure……..……..8

Figure 3-8 TTX (left), C20 FICAS (right)……..……9

Figure 4-1 LRV Geometry……10

Figure 4-2 Sidewall face sheet……11

Figure 4-3 Sidewall inner frame……..11

Figure 4-4 Roof……..…… 11

Figure 4-4 Roof inner frame……11

Figure 5-1 – 5-5 Materials - E-glass, Carbon, Al Honeycomb, Nomex, Foam……..13

Figure 5-6 Young's Modulus of materials…….. 14

Figure 5-7 Density of materials……14

Figure 5-8 Connector Section……..……15

Figure 5-9 Example of connections……15

Figure 5-10 Different type of connectors Figure 6-1 Buckling of I beam……15

Figure 6-1 Buckling of I beam……..……16

Figure 6-2 Composite Layup……17

Figure 6-3 Output node coordinates for the mode shapes……..18

Figure 6-4 Adding Imperfection to the model……..……18

Figure 6-5 Load and boundary conditions in case of buckling……..……19

Figure 6-6 Wind load……19

Figure 6-7 Boundary conditions……..20

Figure 6-8 Load as uniform pressure……20

Figure 6-9 ABAQUS Module……21

Figure 6-10 Master and slave surface side wall panel……22

Figure 6-11 Master and slave surface roof and side wall……..22

Figure 6-12 Element type…… 23

Figure 6-13 Mesh Controls……..23

Figure 6-14 Meshing using quad-dominated elements……24

Figure 6-15 Nomenclature of elements……..24

Figure 6-16 Meshing using S4R elements and S3R elements ……25

Figure 7-1 – 7-7 Buckling Analysis Eigen Value in Mode 1……26

Figure 7-8 Eigen Value Mode 1……..27

Figure 7-9 – 7-10 LPF vs Arc-Length –Steel, Carbon-Al……..28

Figure 7-11 – 7-12 F.O.S vs Displacement – Steel, Carbon –Al……29

Figure 7-13 – 7-15 Dimension Change……30

Figure 7-16 – 7-17 Sequence Change……30

Figure 7-18 – 7-19 Fastener configuration……31

Figure 7-20 – 7-27 Wind Load Stress……..33

Figure 7-28 – 7-34 Wind Load Deformation……34

Figure 7-35 – 7-36 Stress Sequence change……35

Figure 7-37 – 7-38 Deformation Sequence change……36

Figure 7-39 – 7-45 Natural frequency modes…….. 38

Figure 7-46 – 7-47 Natural frequency sequence change……39

Figure 8-1 Emission formula……41

Figure 9-1 Hexagonal layout……..42

Figure 9-2 Shape of different stiffeners……42

Figure 9-3 Car body……42

Appendix Figure B-1 Mesh size 0.8 inch……45

Figure B-2 Mesh size 0.5 inch ……..45

List of Tables

Table 5-1 Material Properties……..13

Table 5-2 Core Material Properties……14

Table 7-1 Buckling analysis eigenvalue mode 1 and F.O.S Comparison……..……27

Table 7-2 Dimension change from 0.2 to 0.15 eigenvalue mode 1 and F.O.S Comparison……31

Table 7-3 Sequence change to symmetric layup eigenvalue mode 1 and F.O.S Comparison……..……31

Table 7-4 Fasteners spacing change effect on eigenvalue mode 1 and F.O.S Comparison……..……..32

Table 7-5 Mass of side wall Comparison……..……...32

Table 7-6 Wind load Stress, Deformation and F.O.S comparison……..……..…36

Table 7-7 Wind load Sequence change to symmetrical layup Stress, Deformation and F.O.S…… comparison……..……..……..37

Table 7-8 Natural frequency Modes comparison……..……..…40

Table 7-9 Natural frequency sequence change to symmetrical layup modes comparison…… 40

Chapter 1

Introduction

A railroad car is a vehicle used for carrying cargo and passengers. A railway carriage can be divided into three main assemblies a) car body structure b) the running gears c) equipment like interior and propulsion, etc. The car body is a relatively long and slender tube-like structure and the main function of a car body is to provide passengers with sufficient safety and comfort. The car concept is limited to only the load carrying the structure of the vehicle. Modern rail vehicles are designed as lightweight structures with the aim to minimize mass and thus operational energy demand. The use of composite materials in vehicle structure could reduce the weight and thereby the fuel consumption without compromising the stiffness of the structure. [1] [2]

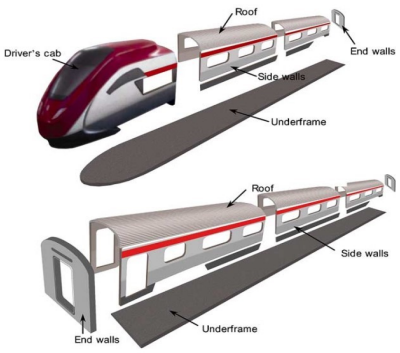

Figure 1-1 Car body [1]

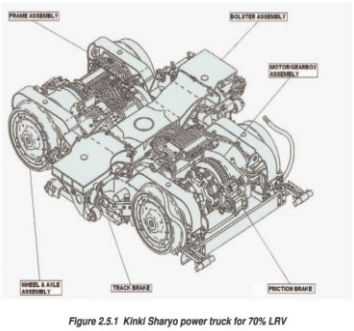

Figure 2.5.1 Kinki Sharyo power truck for 70% LRV

Figure 1-2 Running gears [3]

Figure 1-3 Equipment [4]

So, it is very important to define requirements which must be fulfilled in order to design and manufacture a viable vehicle [1] [5]. Some of the requirements summarized below:

a) The vehicle structure should not collapse during typical operational loads.

b) The weight of rail vehicle should be limited to keep the wear on wheels, breaks, and axles low.

c) Car body should be designed to limit the risk of fire ignition due to electrical malfunction and arson.

d) Car body should be safe to operate in different climates and temperatures.

e) Deformation in any part of the car body shall not exceed 90% of yield value of the material being used.

Due to the scope of this thesis, the car body functions and requirements considered and discussed are limited to Low Weight, Strength, Stiffness, Manufacturability and Energy Consumption.

Mild Steel or power pressed aluminum profiles are the most commonly used material throughout the car body because of their low densities and excellent range of properties. Recently, composites, or fiber – reinforced composites are being used by rail manufacturing industries. The most frequently used reinforcing fibers are carbon, glass, and aramid.

This Thesis research deals with the two loads on the side wall of a railroad car. First, Car Body Side Wall Panels under dead load of the roof and second, Wind load on the Side of the wall. In the case of the composite, the dead load of the roof is different than in the case of mild steel. In the case of second analysis, Wind load is acting on the one side of the train at the speed of 40.3 mph. These loads give rise to high stress and moments. An analysis is conducted by comparing the material change from Mild Steel to Composite.

Chapter 2

Motivation

The railroad car is a good mode of transportation and to make it more reliable it is necessary to keep improving its design. The railroad car structure primary function is to carry loads that act directly on it. So, it is highly desirable that structure should be able to bear load during its operation. Side Walls are the most important component which takes the weight of the roof, AC unit and wind loads on side of the car body and ensures the safety of occupants. Lowering the energy usage in railroad rolling stock often requires new weight-out strategies. So, the main motivation is to replace the heavy panel's materials –mild steel with advanced composite panels which can significantly cut weight while establishing great stiffness and strength and delivering vital benefits like reducing the complexity of structure. Reduced weight lower initial inertia, allowing achieving higher speeds efficiently and quickly. This will further reduce wear and load on the axle. There are various composites available today to choose from to meet specific requirements. The consequent use of the most suitable material for the most appropriate application opens up a large potential for hybrid designs in lightweight construction. [6]

Objective

The main focus of the methodology developed is on the lightweight design of structures while simplifying the construction to reduce manufacturing and assembly times. Increase in the lifecycle cost saving and durability of a product is a prominent positive factor to use composite. The main aim of the work is to compare and correlate results obtained from the analysis of various types of materials currently used for Railroad Car body production. An Alternative design change has also been suggested for the Side Wall panels including structural stiffeners which would not only have an impact on reducing the weight, but also the cost of the Car body. Composite Material is recommended for the safe operation of Sidewall panels under dead load of roof and wind load replacing the conventional material without compromising the safety.

Chapter 3

Literature

3.1 History

The following figure shows the timeline of the body shell evolution from the initial wooden construction to the present-day hybrid construction. [3]

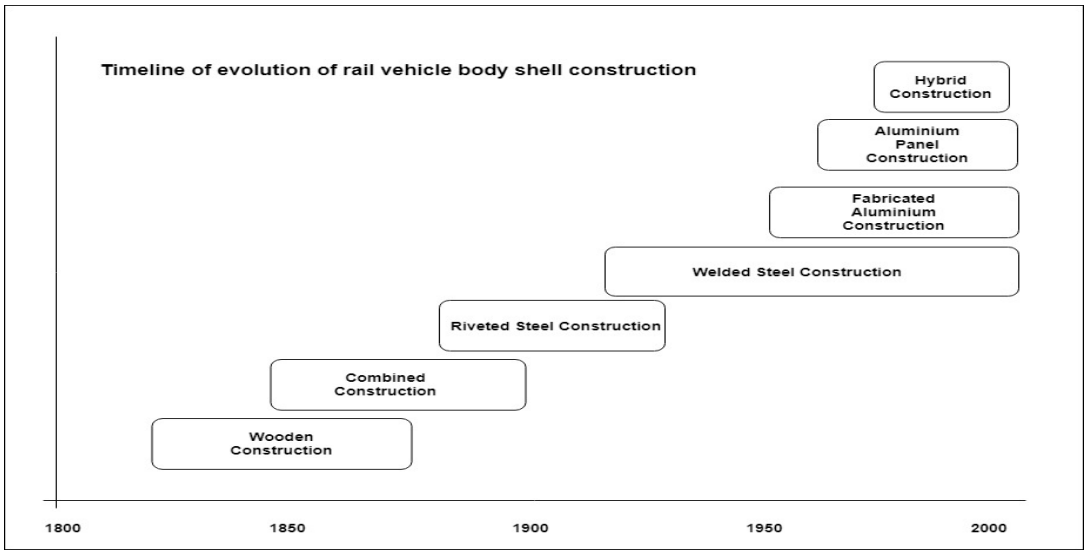

Figure 3-1 Timeline of the body shell evolution [3]

3.2 Sandwich Structures

Sandwich structures consist of three main elements, two outer faces, or skins, and a center core.

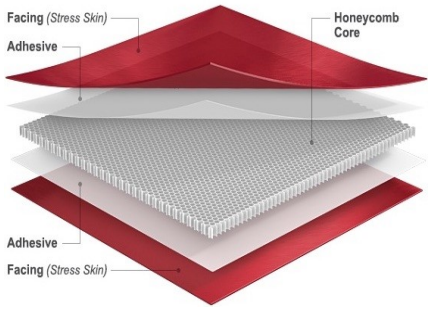

Figure 3-2 Sandwich structures [7]

The face materials are common fiber reinforced plastics or sheet metals, while the core materials are usually of lower density such as honeycomb structures, polymer foams, and balsa wood. There are many combinations that can be made to meet specific requirements.

3.3 Function of sandwich structures

The sandwich structure function in a similar way as an I-beam in bending, the outer faces are there to withstand the compressive and tensile stresses much like flanges of an I-beam and the center core carriers most of the shear stresses. [7]

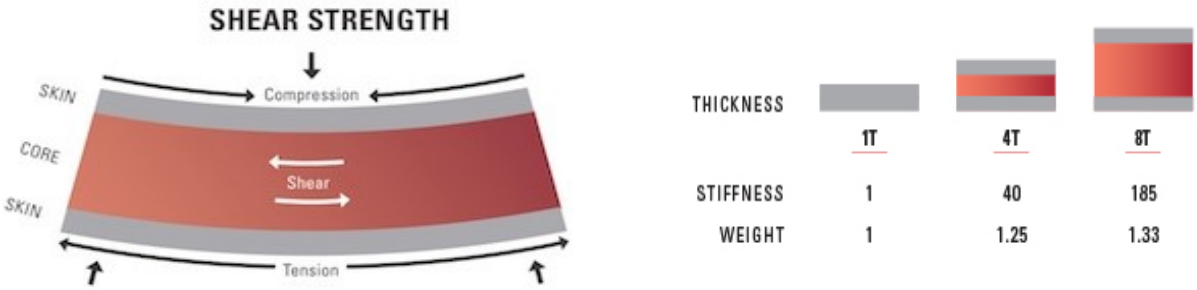

Figure 3-3 Sandwich structure strength [7]

Sandwich structure stiffness increases exponentially as the thickness of the core increases.

3.4 Application of Honeycomb Panels

1. Building products - wall cladding, ceiling, canopies, and interiors,
2. Commercial - doors, platforms, fixtures because of elevated mechanical properties like moisture, chemical & impact resistance as well as vibration dampening,
3. Ground Transportation – lightweight solution – walls, doors, floors, seating bulkhead, ceilings etc.,
4. Marine & Recreation – sporting goods, boat decks, partitions, hatches

Figure 3-4 Use of Honeycomb panels in different industries [7]

3.5 Composites

A composite material is a material having two or more distinct constituent materials or phases. The material can be recognized by composites only when the constituent phases have significantly different physical properties. In case of metals, the constituent's phases often have nearly identical properties. A composite material has two phases: one is called as a reinforcement which is stiffer & stronger, and the less stiff, continuous phase is called the matrix. Composites have been fabricated to improve mechanical properties such as a) strength b) stiffness c) toughness d) high-temperature performance. The strength mostly depends on the geometry of the reinforcement. [8]

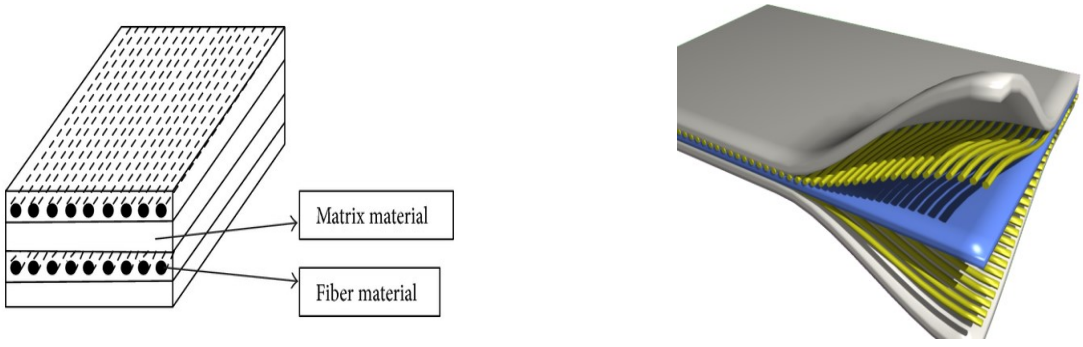

Figure 3-5 Fiber and Matrix material [9]

3.6 Classification of Composite

A fiber is characterized by its length being much greater than its cross-section dimensions. Particle reinforced composites are sometimes referred to as particulate composites. Fiber reinforced composites are called fibrous composites. Fibers, because of their small cross-sectional dimensions, are not directly usable in engineering applications therefore embedded in matrix materials to form fibrous composites.

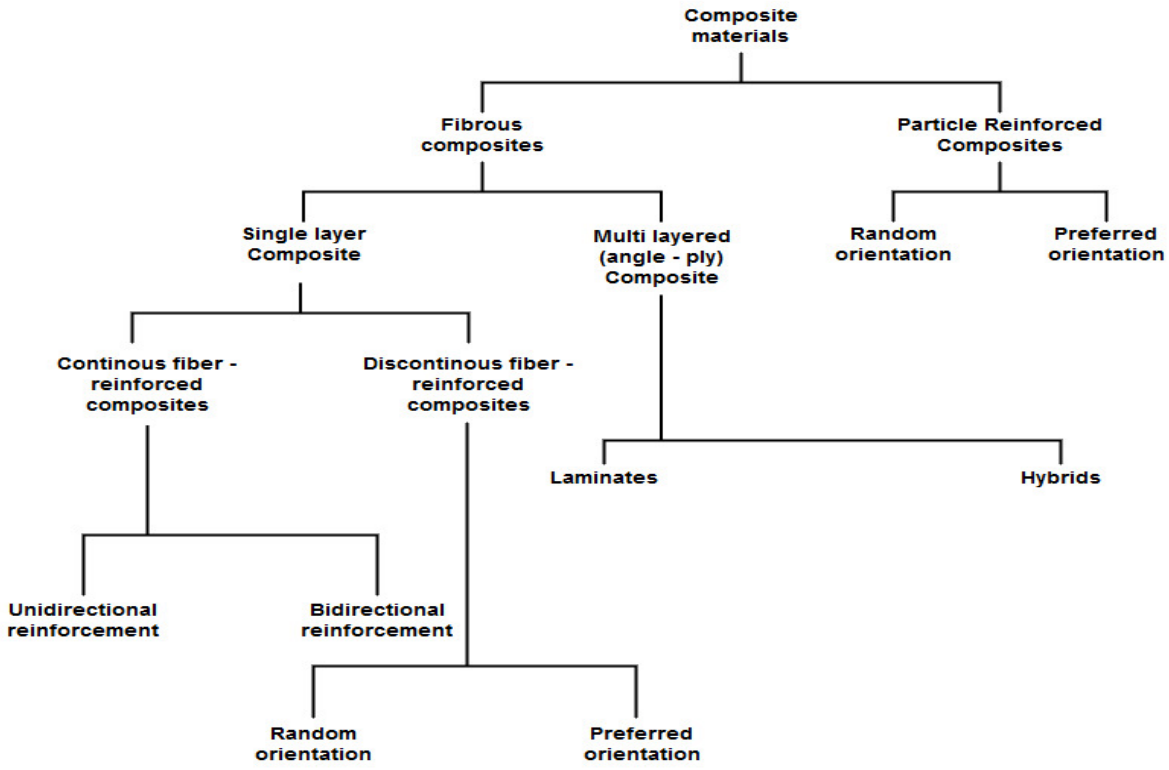

Figure 3-6 Classification of composite [8]

The matrix serves to bind the fibers together, transfer loads to the fibers, and protect them against environmental attacks and damage due to handling. In discontinuous fiber reinforced composites, the load transfer function of the matrix is more critical than in continuous fiber composites. Composite has a high strength-weight ratio and controlled anisotropy features that makes it most widely used in the Transportation industry. The lamina is made up of a number of fibers, i.e. the reinforcement (e.g. glass or carbon fiber) and a matrix material, commonly a polymer. The matrix surrounds the fiber and keeps them in place that results in high strength and rigidity in the fiber direction, while in the transverse direction, it is the strength and

stiffness of matrix that dominates the mechanical properties of the laminate. This lamina is, therefore, a highly orthotropic component. Adding composite face sheets to the sandwich structure gives added complexity to the problem but also added design space. The composite face sheets can be engineered to optimize the directional properties of the component. [8]

The railroad cars which are currently using sandwich structures are: -

3.7 The Korean Tilting Train eXpress (TTX)

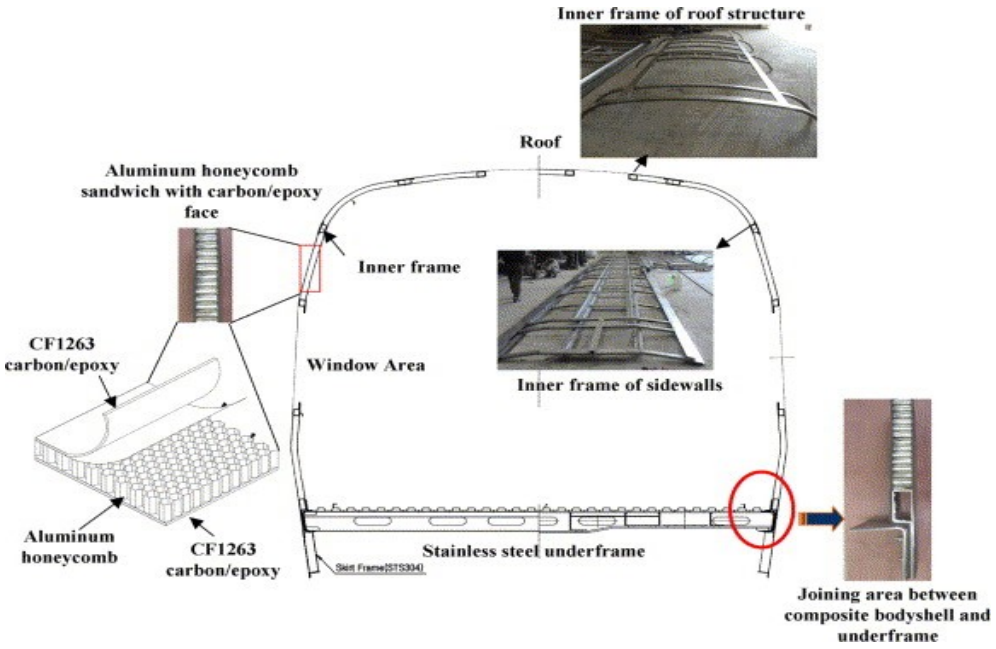

Figure 3-7 Korean Tilting Train body structure [10] [11]

The TTX was designed to run at 200km/h and is composed of four motorized cars and two trailers. To reduce the wear on the tracks the TTX upper body was constructed of a lightweight sandwich structure with a supporting steel inner frame. The door frame is manufactured from conventional stainless steel giving a low center of gravity thereby increasing stability during curve negotiation. The steel door frame also provides increased stiffness against global bending. The sandwich structure elements consist of carbon fabric/epoxy pre-pregs for the faces and an aluminum honeycomb core. The entire car body is manufactured as one single structure. This was accomplished by means of large-scale auto-clave. A large mold was built in which the outer face was first laid out. The outer face was then cured in the autoclave. Secondly, the inner frame and honeycomb core was placed on top of the outer skin. The core and skin

were bonded by use of an adhesive. After this step followed lay-up of the inner face. Lastly, the entire structure was cured in the autoclave after appropriate vacuum bagging. By constructing the entire car body as one structure weak links between panels are eliminated. The sandwich structure reduced the upper car body weight by 39% compared to a stainless-steel car body. The total weight reduction, including underframe, was 28%. [10]

Figure 3-8 TTX (left), C20 FICAS (right) [10]

3.8 C20 FICAS

Operating speed of this railroad car is 80-90 km/h. Stainless steel is used for inner frame and face sheets and PMI foam is used as the core.

3.9 Different types of the body shell

3.9.1 Fabricated Body Shell

Structural parts are manufactured by joining elements usually made of same material.

3.9.2 Panel Construction of Body Shell

This construction consists of each part made of only one material serving several functions.

3.9.3 Hybrid Body Shell

Hybrid body shell consists of combined construction that means body shell is made up of different materials with specific properties as desired for the part. The vital purpose of this type of construction is to reduce weight. [12]

Chapter 4

Geometry

Railroad Car Wall Assembly consists of two panels and several Stiffeners. The Geometry model of the wall is created using SolidWorks V17. [13] [4]. IPS Unit system is used throughout the modeling and analysis. Instead of modeling a full model, it is understandable to use symmetry. Both symmetric and full shell model is designed but the only symmetric model is used for analysis. ABAQUS software is used for simulation needs. The full wall face sheets and inner frame dimensions are 330 in * 125 in and 2 in * 1.2 in. The distance between the wall face sheet is 1.2 inch and inner frame cross-sections used for the study is Rectangular. A standard wall face sheet thickness is 0.2 in. [11]. Initial value used for the stiffeners thickness is 0.08 in. The inner frame is added to increase the bending stiffness [14]. The roof is 11-inch-high, and thickness is 0.5 inch. [15] [16] [17]

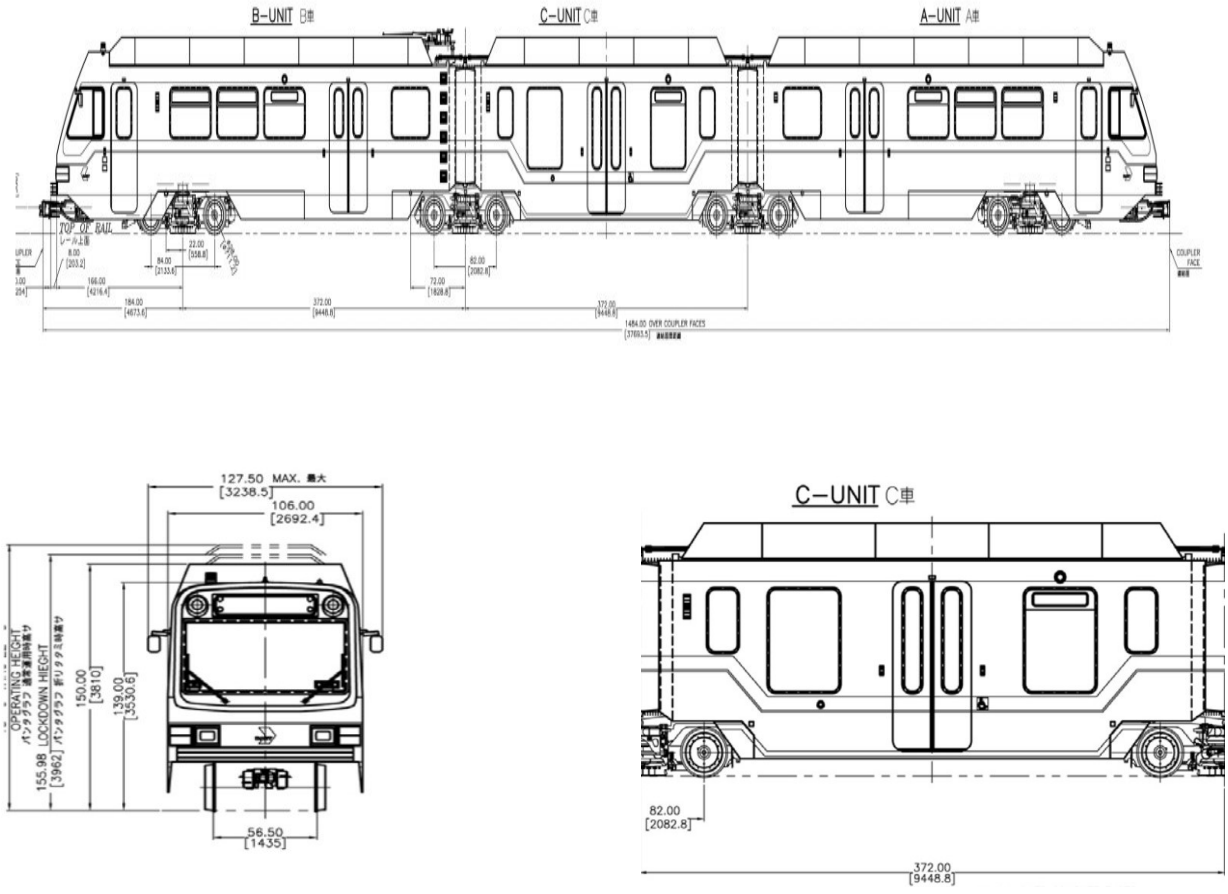

Figure 4-1 LRV Geometry [15]

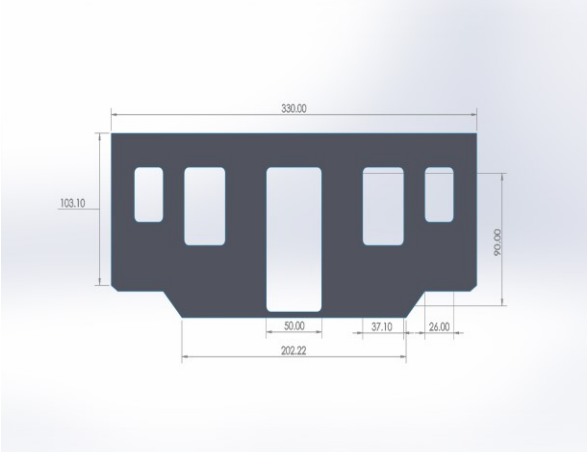

Figure 4-2 Sidewall face sheet

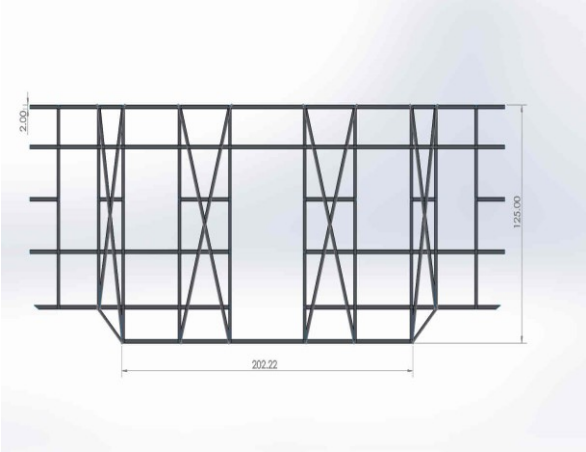

Figure 4-3 Sidewall inner frame

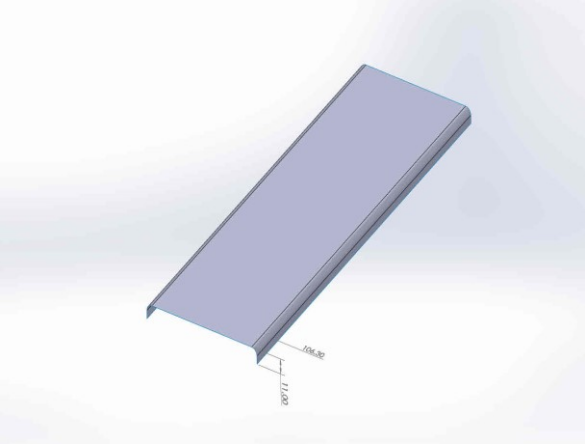

Figure 4-4 Roof

Figure 4-4 Roof inner frame

Chapter 5

Materials

This chapter discusses the isotropic and composite materials that are considered in this analysis. Isotropic materials Mild Steel and Aluminum and composite materials E-glass and Carbon are used in the analysis.

5.1 Mild Steel

It is a steel containing small percentage of carbon. It is also called as “low carbon steel”. It is typically more ductile, Machinable and weldable than other steels and high carbon. It is being used in wide applications such as Automobiles, pipelines, steel frame buildings, fencing etc. [8]

5.2 Glass Fiber

Glass fiber is reinforcing fiber with advantages of high strength and low cost. For structural composites, the most commonly used types of glass fiber are E-glass and S-glass. Glass fiber has poor abrasion resistance, which reduces their usable strength. Compared to other reinforcing fibers such as carbon, Kevlar, and boron glass fibers have a lower modulus. Glass fiber is available as a dry fabric or prepreg material. [8]

5.3 Carbon Fiber

Carbon/graphite fibers are used in the fabrication of high-performance polymer-matrix composites because of its high – strength and high modulus. These fibers also have higher resistance to corrosion when compared to other fibers. They are now being used in aerospace applications, sporting goods, civil infrastructure, automotive etc. Carbon fibers properties can be altered easily by controlling their structure through manufacturing process (e.g., by heat treatment temperature). Fibers are available in continuous, chopped, woven fabric and mat forms. [8]

5.4 Epoxy Resin

Epoxy Resin is a viscous liquid and the viscosity is a function of the degree of polymerization 'n'. They are widely used as structural adhesives and resins. They have high strength, low shrinkage, high modulus, great chemical resistance and are very easy to process. [8]

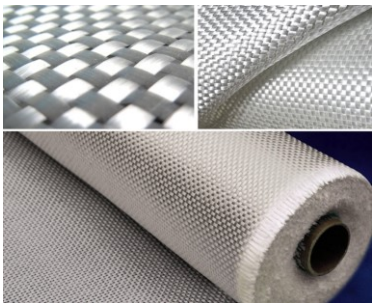

Figure 5-1 E-glass [28] [18]

Figure 5-2 Carbon [18]

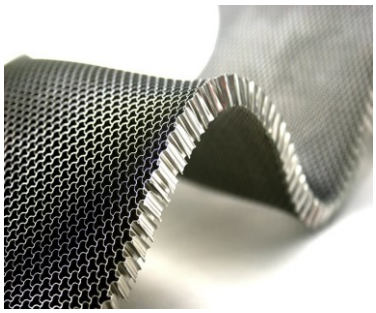

Figure 5-3 Al – Honeycomb [18]

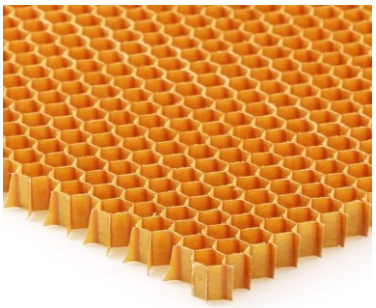

Figure 5-4 Nomex [18] [19]

Figure 5-5 Polyurethane foam [18]

Physical Properties	Mild Steel	E-glass/Epoxy	Carbon/Epoxy	Units
E1 e10^5	304.57	65.26	213.2	Psi
E2 $e10^5$	304.57	15	14.93	Psi
E3 $e10^5$	304.57	15	14.93	Psi
G12 $e10^5$	114.57	7.25	10.15	Psi
G13 $e10^5$	114.57	7.25	5.36	Psi
G23 $e10^5$	114.57	5.57	5.36	Psi

V12	0.28	0.3	0.27	
V13	0.28	0.3	0.27	
V23	0.28	0.4	0.54	
Density	0.281	0.072	0.0538	$\frac{lb}{in^3}$

Table 5-1 Material Properties

Physical Properties	Aluminum Honeycomb	Nomex Honeycomb	Poly Foam	Units
E1	1200	4482	5100	Psi
E2	190	4482	5100	Psi
E3	185068.2	4713726.5	15900	Psi
G13	43000000	275571.7	14500	Psi
Density	0.0036	0.0017	0.000578	$\frac{lb}{in^3}$

Table 5-2 Core Material Properties

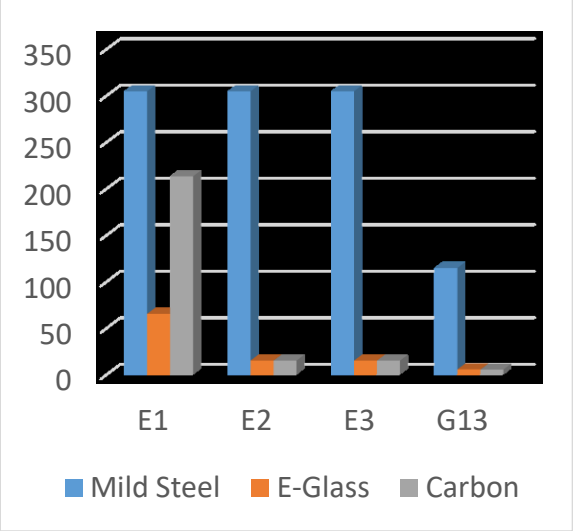

Figure 5-6 Young's Modulus of materials

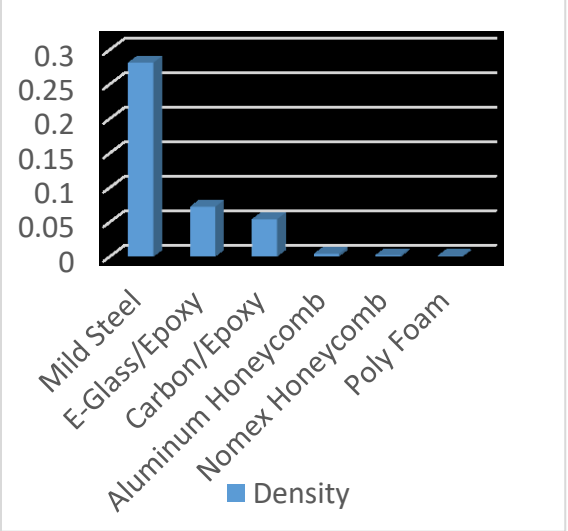

Figure 5-7 Density of materials

5.5 Constraints vs Connectors

Constraints – Partially or fully eliminate D.O.F of a group of nodes and Couple motion with master nodes

Connections – Model actual connections between parts, such as springs, spot welds, hinges, bonds etc.

Types of fasteners – Point based and discrete

Type of Connector 1) Translational Type – Cartesian(None), Join(Displacement), Slide-Plane(U1)

2) Rotational Type – Cardan, Rotation(None), Align(Rotation), Universal(UR2)

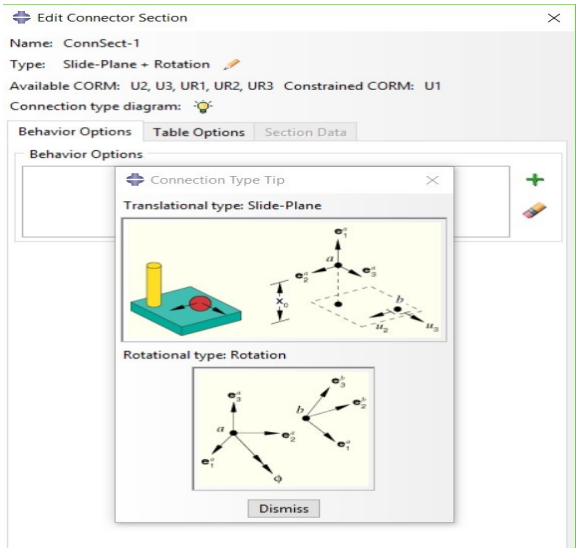

Figure 5-8 Connector Section [20]

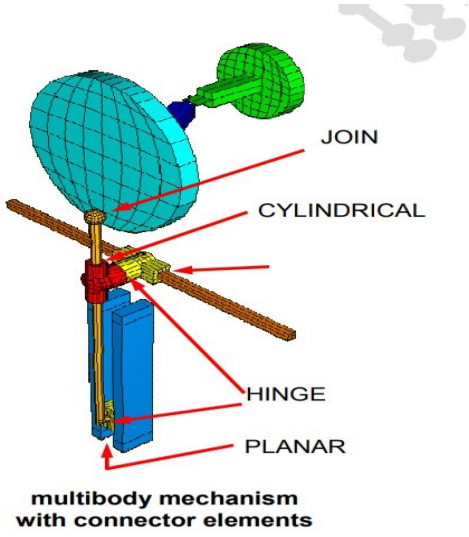

Figure 5-9 Example of connections [21]

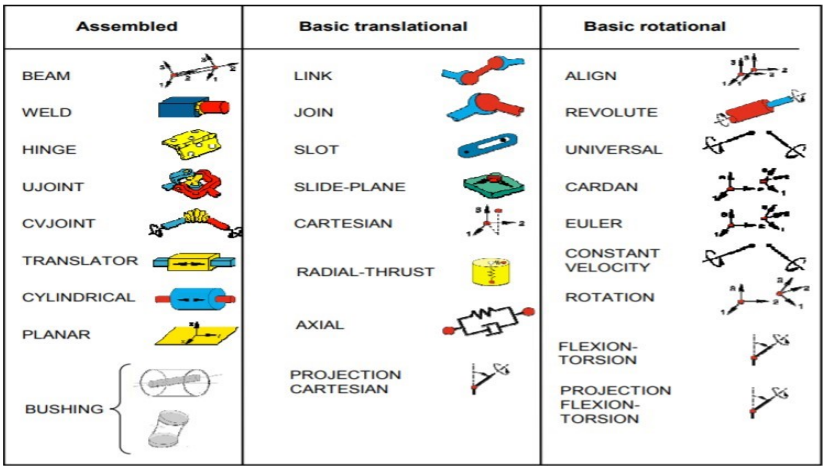

Figure 5-10 Different type of connectors [21]

Fasteners are applied in order to resist delamination or detachment of composite plies. If the model has more than 1000 fasteners, it is better to use point-based because it provides superior performance. [21]

Chapter 6

Loading and Boundary Conditions

Two loading conditions are considered in this chapter. The conditions are buckling of the side wall and bending of the wall due to side wind load.

6.1 Buckling

Buckling occurs as an instability when a structure can no longer support the compressive load. The critical load that will cause the first buckling mode is calculated from the nominal load 1 lbf multiplied by eigenvalue. Each side wall panel is 0.2-inch-thick and 1.2-inch-thick core. Instead of using full model it is understandable to use symmetry. Parts are assembled together in assembly using Tie – Constraints. Fasteners of Radius 0.125 inch is applied to the side wall in interaction module.

Total weight of the Unit – C = 35560 lb. The Structural weight of steel car body is 22% - 25% of the entire vehicle weight. Considering 25%, the weight of the steel car body is 8,890 lb. The calculated mass of the steel roof = 1820 lb. Total load of 1820*386.09 = 702,683 lbf is applied. [22]

6.1.1 Analytic Solution

$$I_{xx} = \frac{(H^3 \cdot b)}{12} + 2 \cdot \left(\left(h^3 \cdot \frac{b}{12} \right) + h \cdot \frac{b(H+h)^2}{4} \right)$$

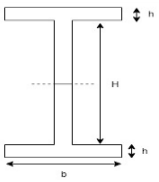

$$P_{cr} = \frac{(\pi^2 \cdot E \cdot I_{xx})}{L^2}$$

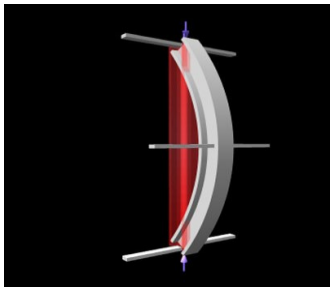

Figure 6-1 Buckling of I beam

6.1.2 Ply Sequence

90	90	45	90	90	0	90	90	-45	90	90	45	90	90	0	90	90	-45

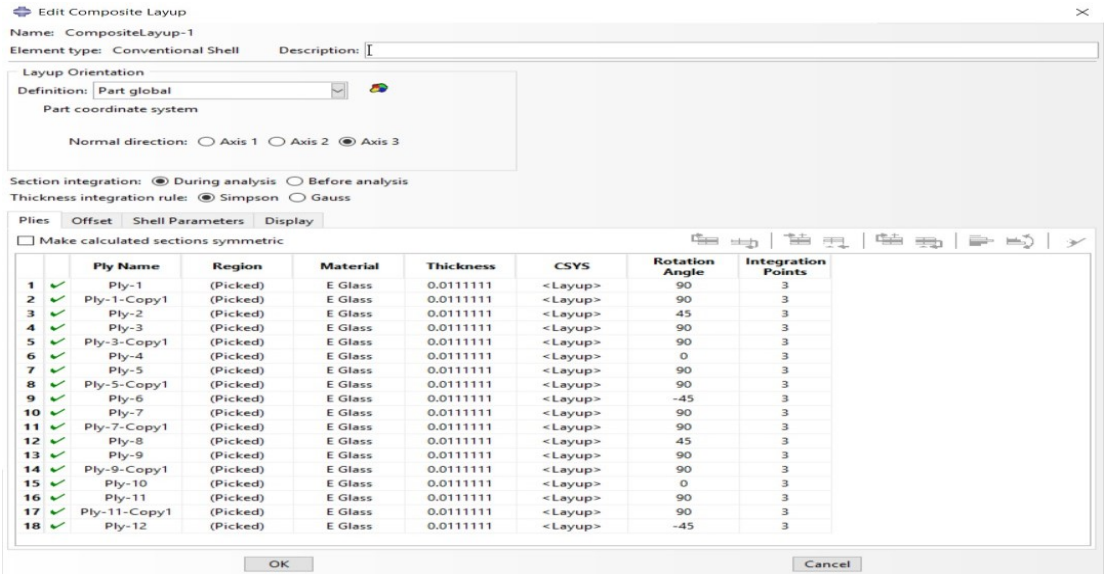

		Ply Name	Region	Material	Thickness	CSYS	Rotation Angle	Integration Points
1	✓	Ply-1	(Picked)	E Glass	0.0111111	<Layup>	90	3
2	✓	Ply-1-Copy1	(Picked)	E Glass	0.0111111	<Layup>	90	3
3	✓	Ply-2	(Picked)	E Glass	0.0111111	<Layup>	45	3
4	✓	Ply-3	(Picked)	E Glass	0.0111111	<Layup>	90	3
5	✓	Ply-3-Copy1	(Picked)	E Glass	0.0111111	<Layup>	90	3
6	✓	Ply-4	(Picked)	E Glass	0.0111111	<Layup>	0	3
7	✓	Ply-5	(Picked)	E Glass	0.0111111	<Layup>	90	3
8	✓	Ply-5-Copy1	(Picked)	E Glass	0.0111111	<Layup>	90	3
9	✓	Ply-6	(Picked)	E Glass	0.0111111	<Layup>	-45	3
10	✓	Ply-7	(Picked)	E Glass	0.0111111	<Layup>	90	3
11	✓	Ply-7-Copy1	(Picked)	E Glass	0.0111111	<Layup>	90	3
12	✓	Ply-8	(Picked)	E Glass	0.0111111	<Layup>	45	3
13	✓	Ply-9	(Picked)	E Glass	0.0111111	<Layup>	90	3
14	✓	Ply-9-Copy1	(Picked)	E Glass	0.0111111	<Layup>	90	3
15	✓	Ply-10	(Picked)	E Glass	0.0111111	<Layup>	0	3
16	✓	Ply-11	(Picked)	E Glass	0.0111111	<Layup>	90	3
17	✓	Ply-11-Copy1	(Picked)	E Glass	0.0111111	<Layup>	90	3
18	✓	Ply-12	(Picked)	E Glass	0.0111111	<Layup>	-45	3

Figure 6-2 Composite Layup

Other Ply-Sequences considered in Buckling, Wind and Modal Analysis are:

Sequence 1 - [90/90/45/90/90/0/90/90/-45] s

Sequence 2 - [90/90/45/90/90/-45/90/90/0] s

6.1.3 Boundary Conditions

B.C 1 – Symmetry along the X-Axis on left

B.C 2 – Simply supported on the bottom

B.C 3 – Free to move in the y-direction on the top

B.C 4 – Constrained in the Z direction

Initially, buckling analysis in the case of E-glass-Al is done and the F.O.S was way too less than in the case of mild steel. So, in order to increase the F.O.S, inner frame thickness is increased from 0.08in to 0.24in rather than increasing the thickness of face sheets because later will decrease the space for passengers. So, in all the cases of composite inner frame thickness is 0.24in. Later I have considered decreasing the

thickness of face sheets to increase the space for passengers and reducing weight further. Also, change in the number of fasteners is considered in addition to the ply sequence change from asymmetric to symmetric. In sequence 1, 45° plies position is changed and in the sequence 2, the position of 0° plies is changed to decrease the stress in 0-degree layers, which in all the cases are failing first. Ply sequence angles are determined using the performance analysis of angle. 90 -degree panels are more dominant to provide more strength in the case of buckling therefore 60-70% are 90-degree panels, 20% are 45-degree panels, rest are 0-degree panels. Thus, the stacking sequence is balanced but asymmetric. Post Buckling analysis which is a non – linear behavior is also considered which takes place in the very short amount of time. A structure may become unstable once load reaches its buckling value. Instability usually pose convergence difficulties and therefore require special non-linear techniques. I have used Arc-Length method to calculate graph of LPF (Load proportionality factor) with respect to arc length. First buckling modes are calculated and saved as a .fil file which is called in second analysis i.e. Riks analysis and this method is used to calculate LPF vs Arc length graph. The imperfection of 10%*t in the first mode and 5%*t in 2nd mode is requested as shown in Figure 6-4 where 't' is the thickness of face sheet and the modes are called from the first analysis as shown in Figure 6-3.

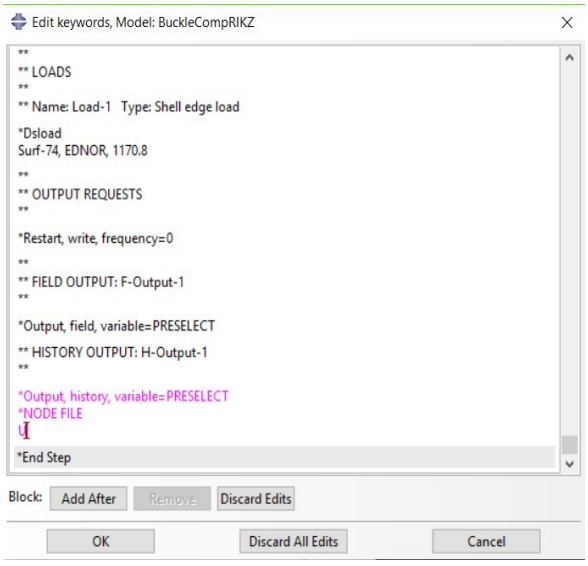

Figure 6-3 Output node coordinates for the mode shapes

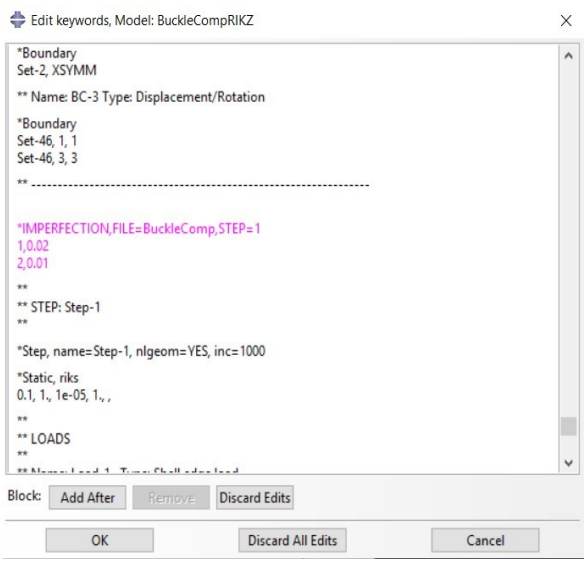

Figure 6-4 Adding Imperfection to the model

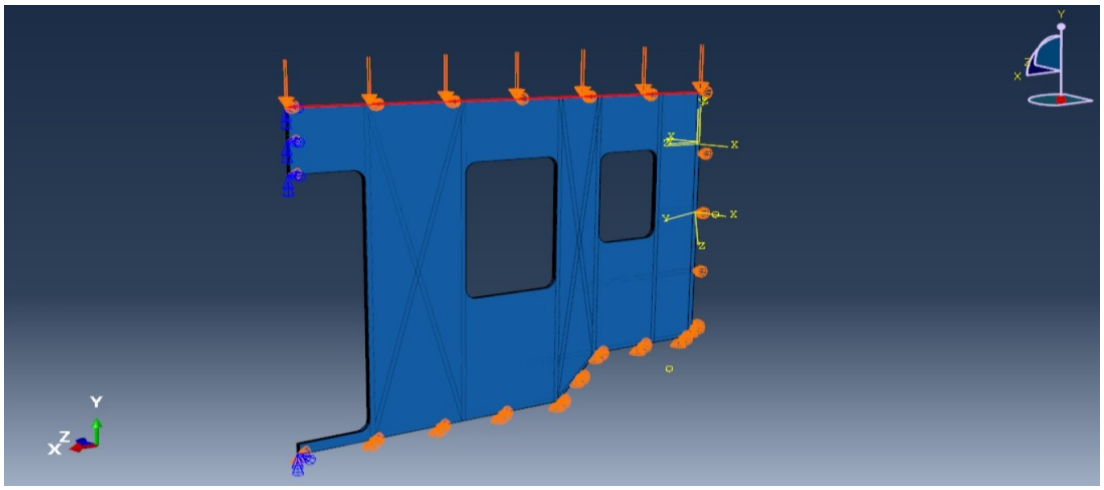

Figure 6-5 Load and boundary conditions in case of buckling

6.2 Wind Load

When the moving air is stopped by a surface the dynamic energy in the wind is transformed to pressure. The dynamic pressure causes the bending of the surface; therefore, it is a vital aspect to consider wind load analysis. [23]

The speed of wind considered for the analysis is 40.3 mph i.e. 709.25 in/sec

$$p_d = \frac{1}{2} \cdot \rho \cdot v^2$$

Where p_d is Dynamic Pressure
ρ is Density of Wind
v is velocity of Wind

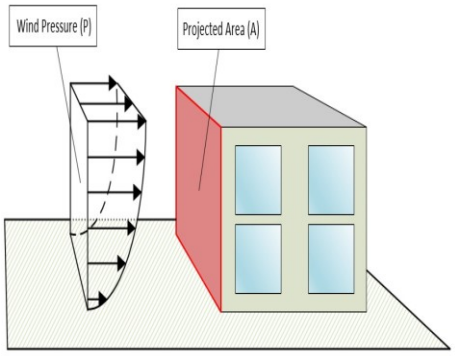

Figure 6-6 Wind load [24]

ρ = 1.0187 * 0.000036 lb/in3

v = 709.25 in/sec

On solving, p_d = 0.0328 psi

B.C 1 – Symmetry along the X-Axis on left

B.C 2 – Clamped on the bottom

B.C 3 – Constrained in the z direction on the right

Roof and opposite side wall are considered in assembly here in order to calculate realistic results.

A wind load of 0.032 psi is applied on one side of the wall in –z direction.

6.2.1 Analytic Solution

Assuming pressure on a clamped plate as an approximate,

For isotropic materials [25]

$$\sigma_m = p \cdot \frac{a^2}{2 \cdot t^2 \left(0.623 \left(\frac{a}{b}\right)^6 + 1\right)} \qquad y_m = 0.0284 \cdot p \cdot \frac{a^4}{E \cdot t^3 \left(1.056 \left(\frac{a}{b}\right)^5 + 1\right)}$$

For composite materials [25]

$$w\left(\frac{a}{2}, \frac{b}{2}\right) = \frac{0.00342 \cdot q \cdot a^4}{\pi^4 \cdot \left(D_{11} + 0.5714 \cdot \left(D_{12} + 2\ D_{66}\right) \cdot \left(\frac{a}{b}\right)^2 + D_{22} \cdot \left(\frac{a}{b}\right)^4\right)}$$

6.2.2 Boundary Conditions & Load

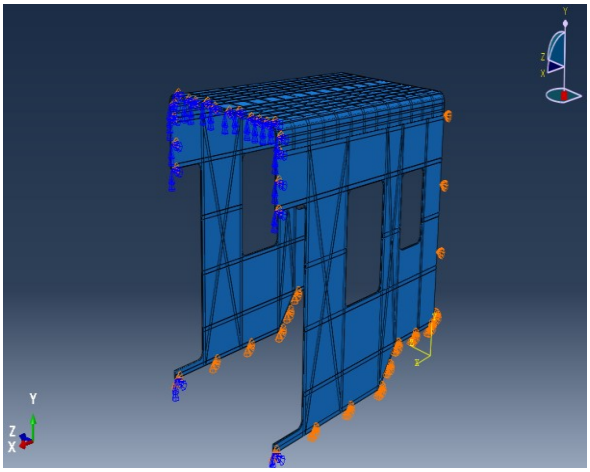

Figure 6-7 Boundary conditions

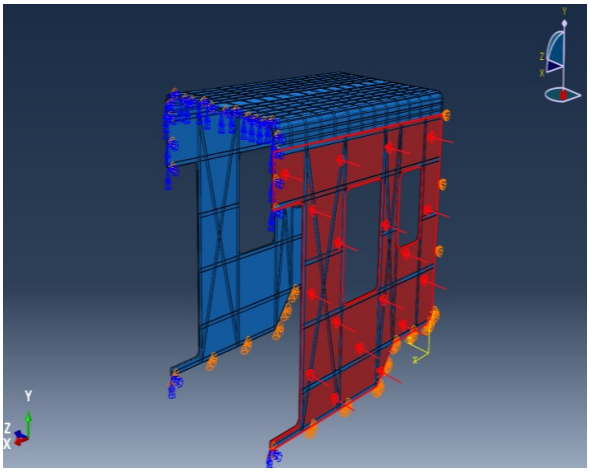

Figure 6-8 Load as uniform pressure

6.3 Simulation

In order to verify the structural integrity of sandwich and conventional walls of railcar ABAQUS was used. The whole ABAQUS procedure can be divided into eight steps. They are as following: Part: The model can be created or imported in this module in various format such as step, vda, iges, Parasolid.

Property: In this module, the material and sections are assigned to the parts either it is a solid, surface etc. A layup in the case of composites is created in this module.

Assembly: Different parts are assembled in this module. Nodes can be easily used to assemble instances

Step: In step manager, a step is created in addition to the initial step. The procedure needs to be assigned, as an example, in the case of buckling Linear Perturbation buckle should be selected. Interaction: Constraints are created in this module that means it needs to define that how the two parts are connected to each other. Fasteners can be created in this module.

Load: Different types of loads can be applied in this section, as an example, Pressure, concentrated force, shell edge load, gravity, etc.

Mesh: Meshing to different instances can be applied in this section. Mesh controls can be assigned to an instance in this module.

Job: Job is created and submitted to this module and result can be viewed in Visualization module.

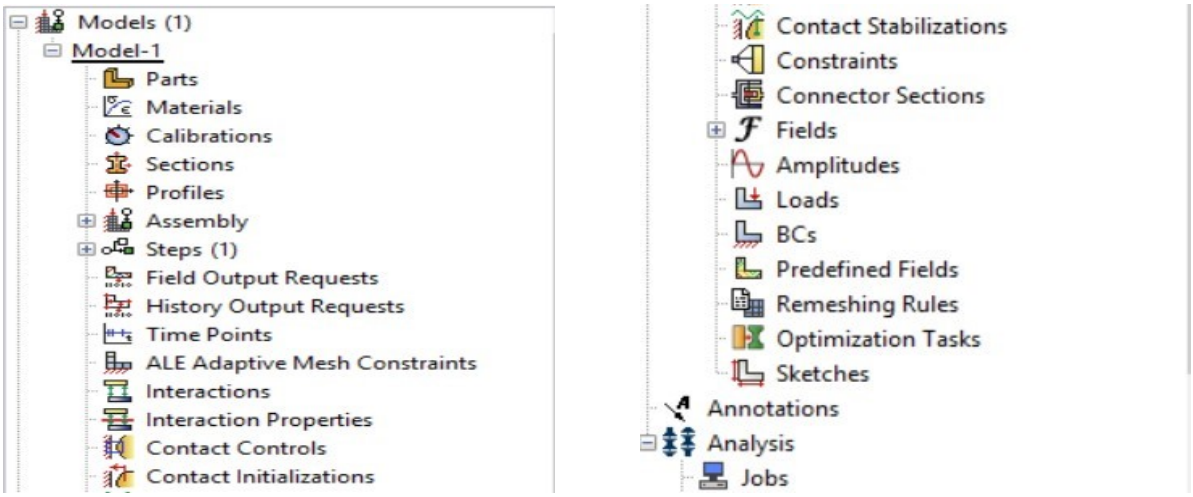

Figure 6-9 ABAQUS Module

6.4 Constraints

Face sheets are selected as master surface and inner frame is selected as slave surface as shown in Figure 6-10 and Figure 6-11.

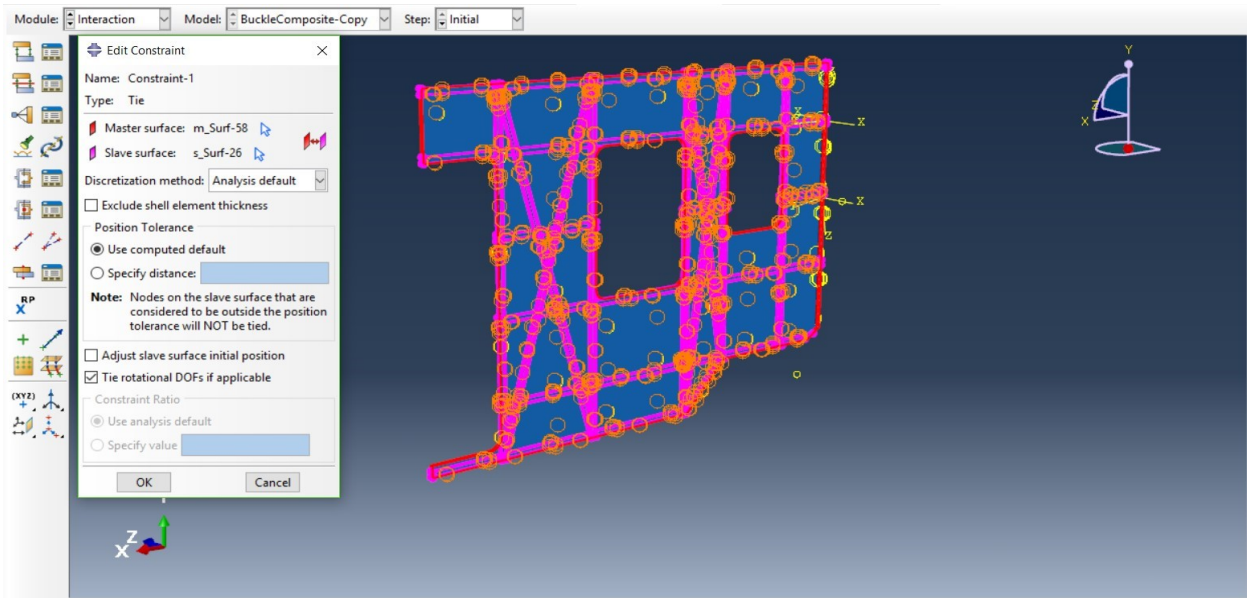

Figure 6-10 Master and slave surface side wall panel

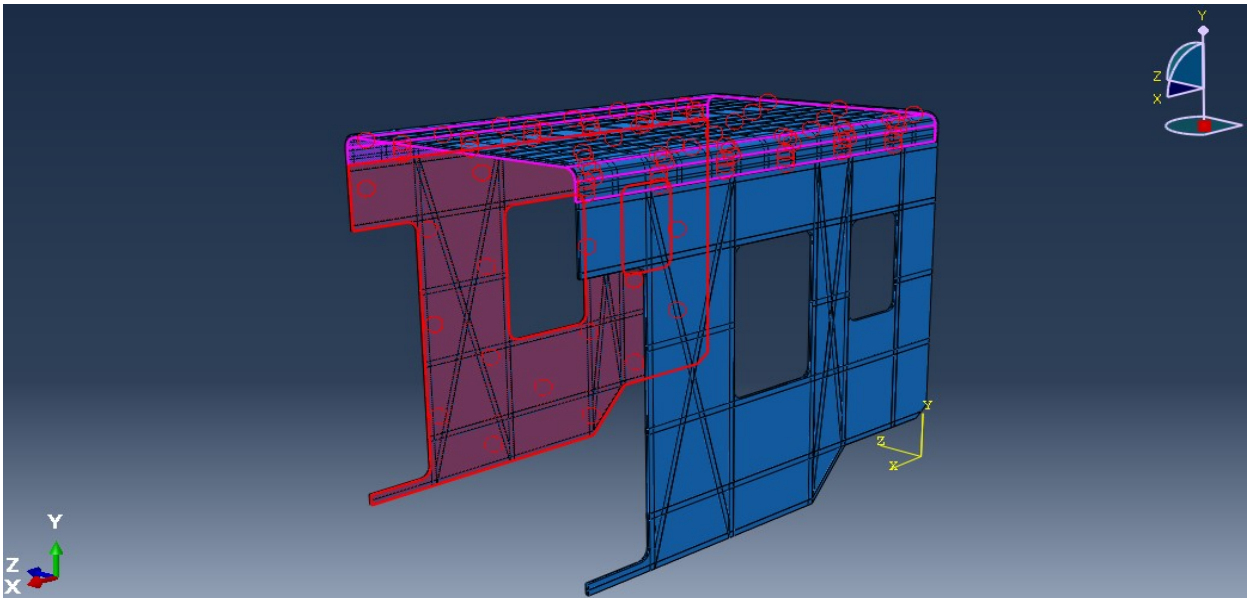

Figure 6-11 Master and slave surface roof and side wall

Step files are imported to ABAQUS in parts and inner frame is stitched together to form a single part. Parts are assembled together in assembly using Tie-Constraints. A tie-constraint ties two separate surfaces together so that there is no relative motion in between them. Material properties are defined in Material Module. Section, thickness, offset surface, the coordinate system is defined in Property Module. In step module, field output and history output are requested. Loads and Boundary Conditions have applied accordingly, and results are obtained after submitting the job.

6.5 Meshing

Meshing was done using the quad dominant method as shown in Figure 6-13. The geometric order is Quadratic and D.O.F per node is 6 as shown in Figure 6-12. Mesh is generated with Shell elements SR. Mesh sizing was selected based on mesh sensitivity analysis which is shown in Appendix B. Mesh size was kept 0.8 inch which is the optimum size for the analysis. [20]

6.5.1 Buckling Analysis

Total Number of Nodes in entire assembly = 321,738

Total Number of Elements in assembly = 98532

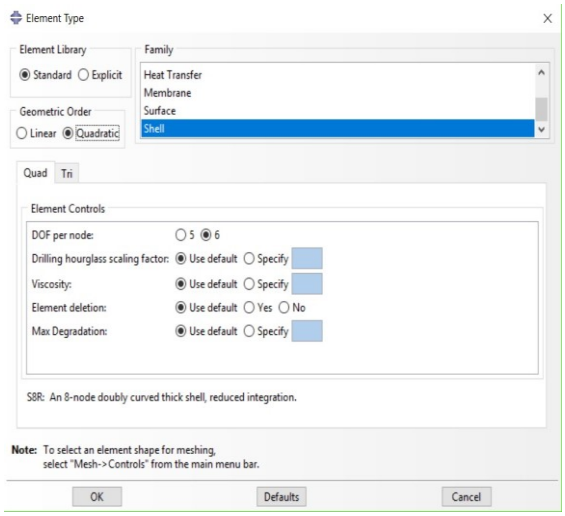

Figure 6-12 Element type

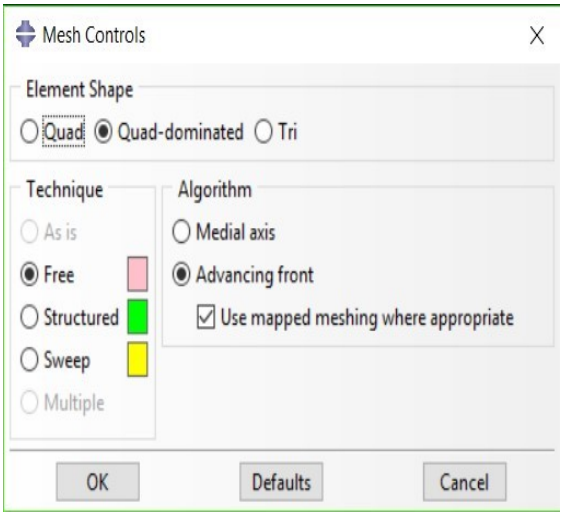

Figure 6-13 Mesh Controls

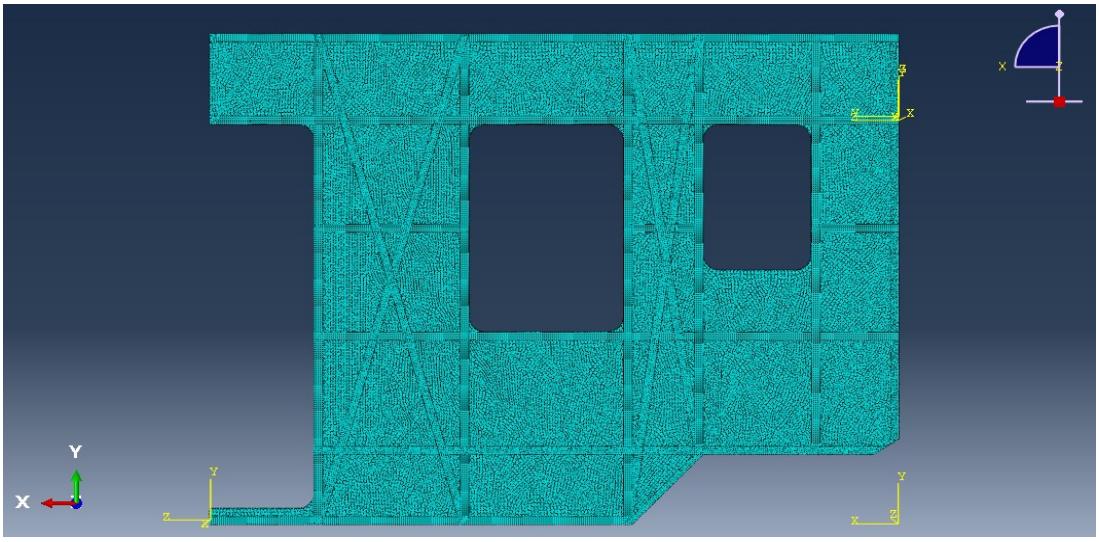

Figure 6-14 Meshing using quad-dominated elements

Element Types & Naming Convention

S8R, STRI65, S4R Elements are used in the Buckling Analysis

Total Number of S8R elements = 94501

Total Number of S4R = 2472

S4R is a 4-node, quadrilateral, stress/displacement shell element with reduced integration and a large strain formulation. [26]

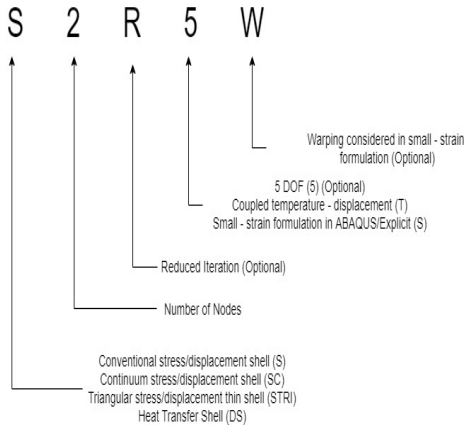

Figure 6-15 Nomenclature of elements [26]

Reduced iteration calculates the stress and strain at locations that provide optimal accuracy and also decrease CPU time and storage requirements.

6.5.2 Wind Load

Total Number of Nodes = 414726

Total Number of Elements = 382612

Linear quadrilateral elements of type S4R = 379494

Linear triangular elements of type S3R = 3118

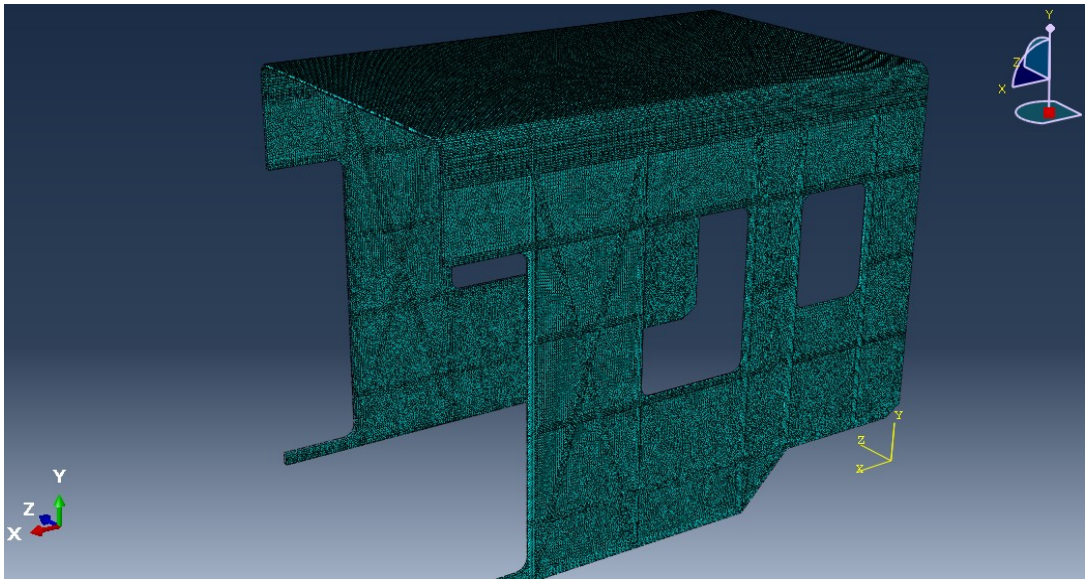

Figure 6-16 Meshing using S4R and S3R elements

6.6 Failure Criteria

In isotropic material, Von Mises stress is used to calculate F.O.S while in the case of the composite, stress in the direction of the fiber is used. In isotropic material, yield stress is considered and, in the composite, when the max stress in the direction of fiber exceeds the strength of the fiber, fiber is considered to be failed. Core failure is also taken into consideration.

Chapter 7

Results

7.1 Buckling Analysis

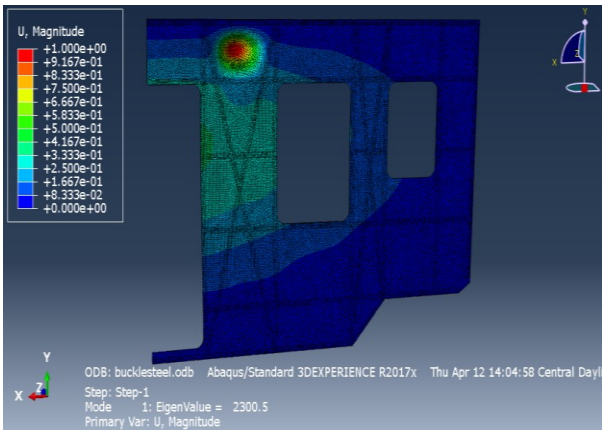

Figure 7-1 Eigen Value in Mode 1 Mild Steel

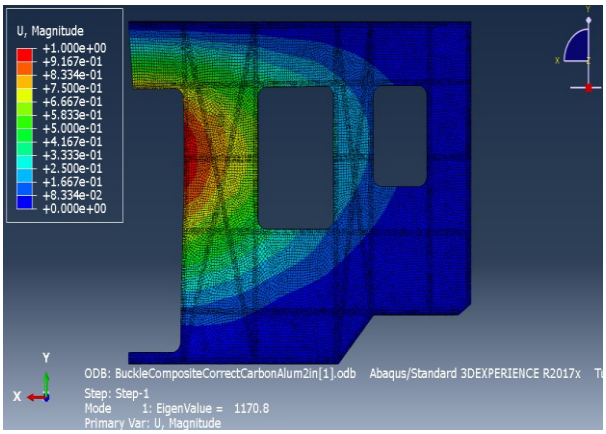

Figure 7-2 Carbon-Aluminum

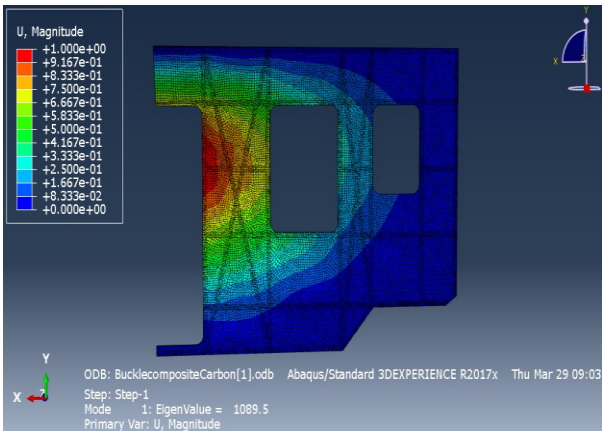

Figure 7-3 Carbon-Nomex

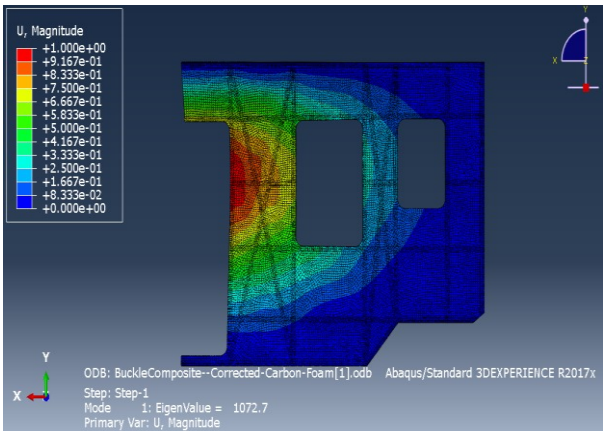

Figure 7-4 Carbon-Foam

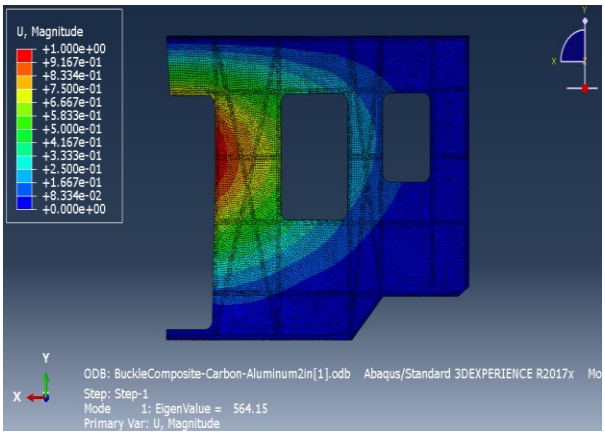

Figure 7-5 E-glass-Aluminum

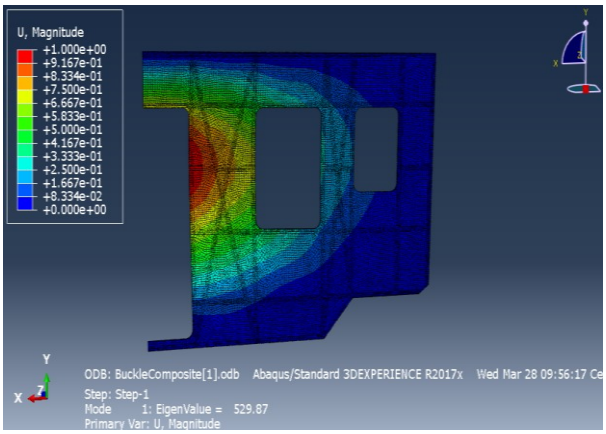

Figure 7-6 E-glass-Nomex

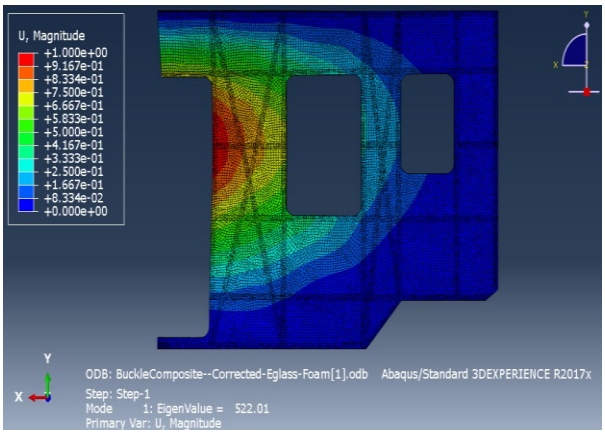

Figure 7-7 E-glass-Foam

Material	Steel	Carbon Aluminum	Carbon Nomex	Carbon-Rigid Polyurethane Foam	E-Glass Aluminum	E-Glass Nomex	E-Glass-Rigid Polyurethane Foam
Eigen Value	2300.5	1170.8	1089.5	1072.7	564.15	529.87	522.01
F.O.S	2.16	5.72	5.32	5.24	2.06	1.94	1.91

Table 7-1 Buckling analysis eigenvalue mode 1 and F.O.S Comparison

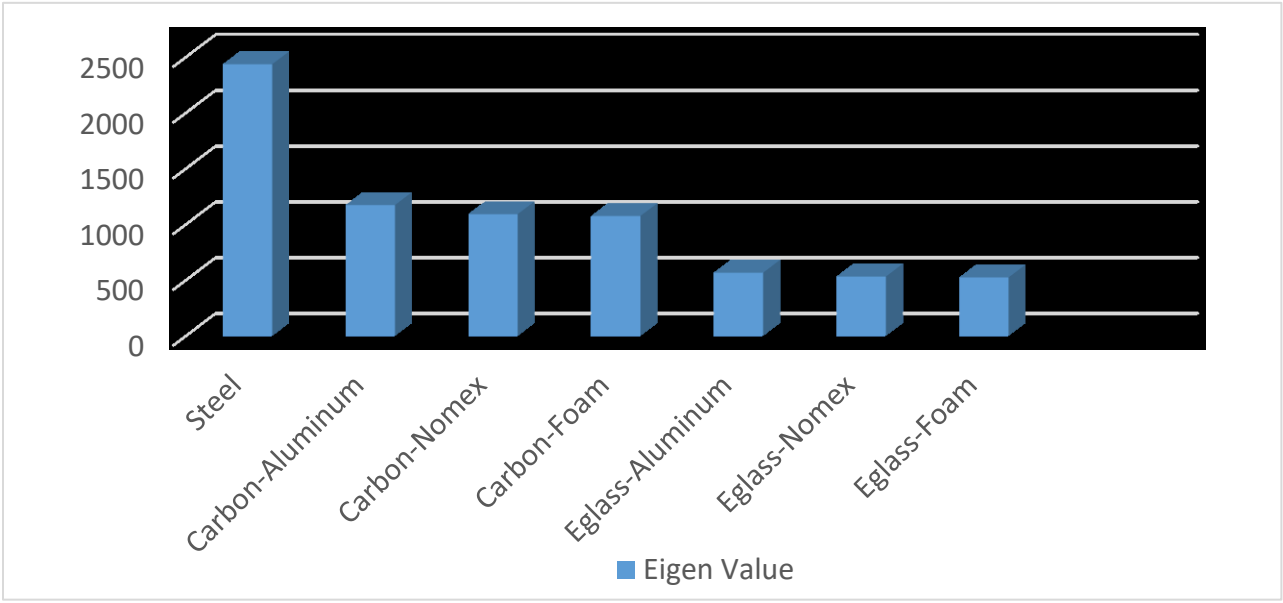

Figure 7-8 Eigen Value Mode 1

7.1.1 Post Buckling

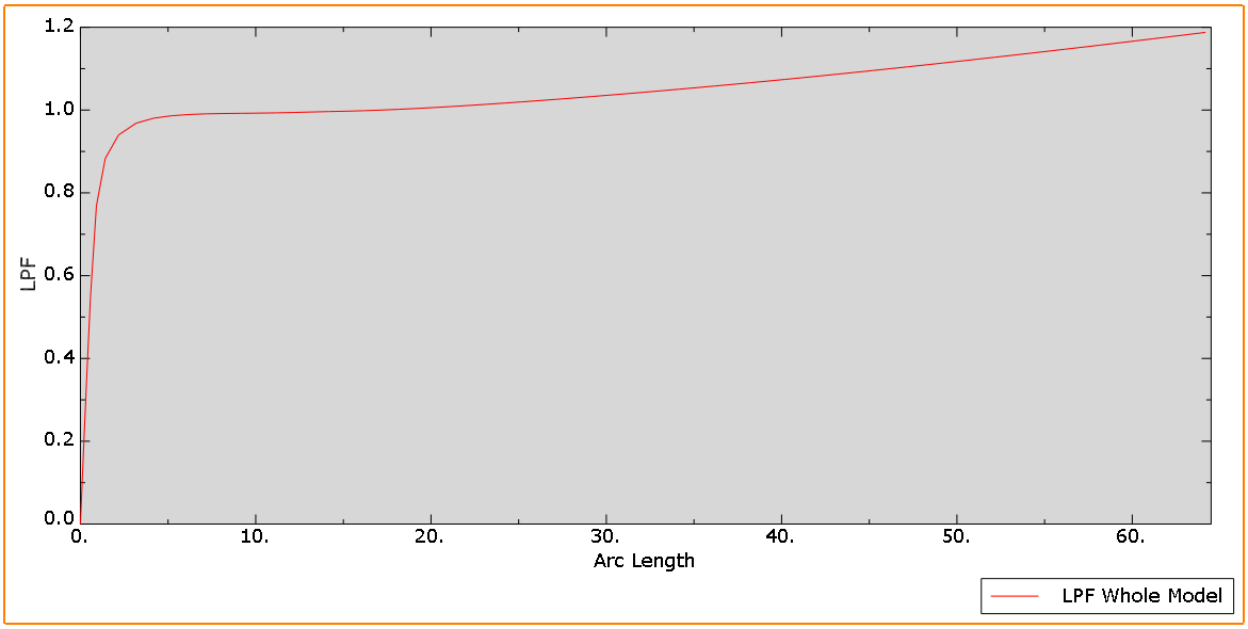

Figure 7-9 LPF vs Arc Length - Steel

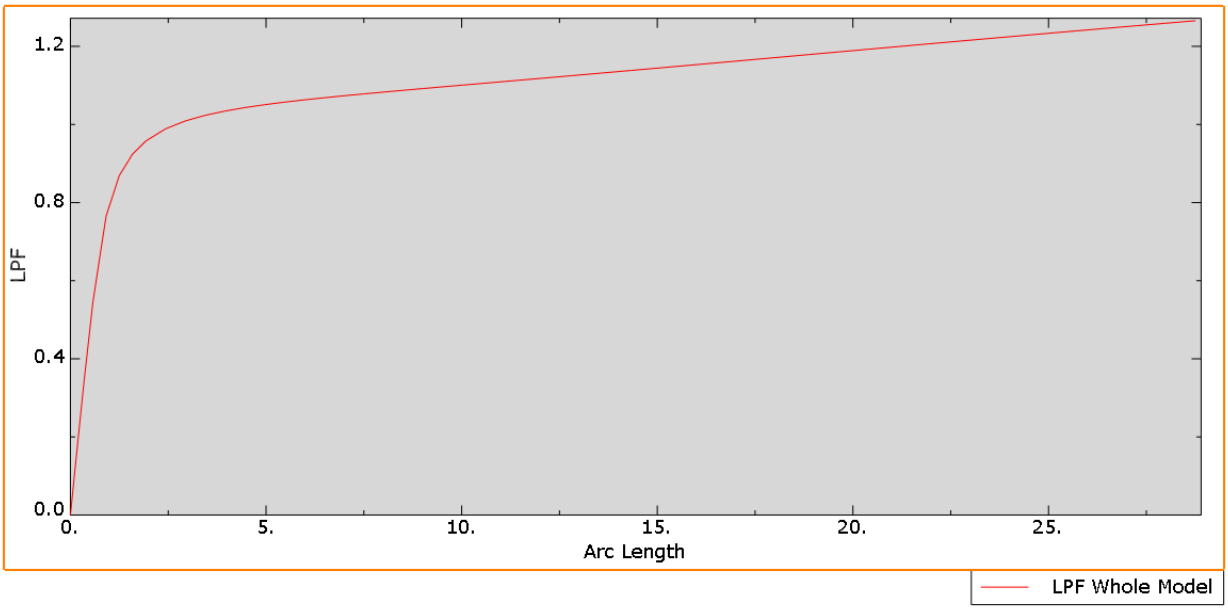

Figure 7-10 LPF vs Arc Length – Carbon – Aluminum

7.1.2 F.O.S vs Displacement

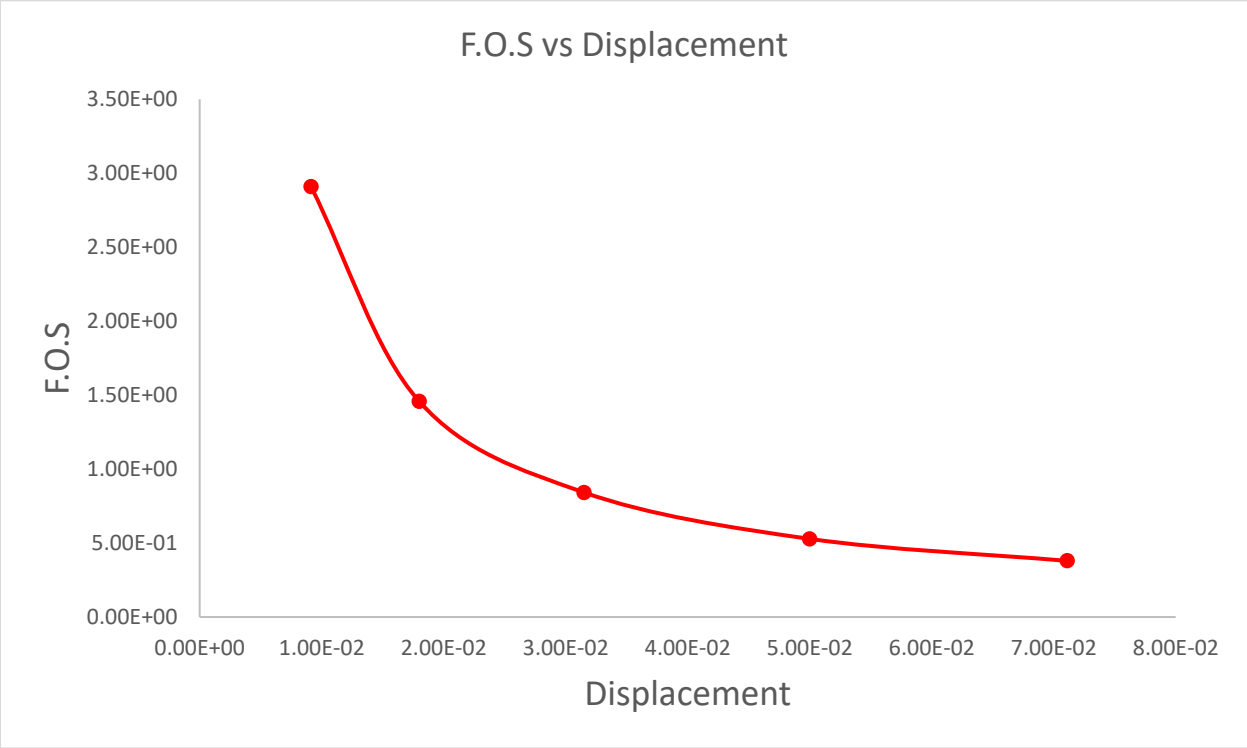

Figure 7-11 - F.O.S vs Displacement - Steel

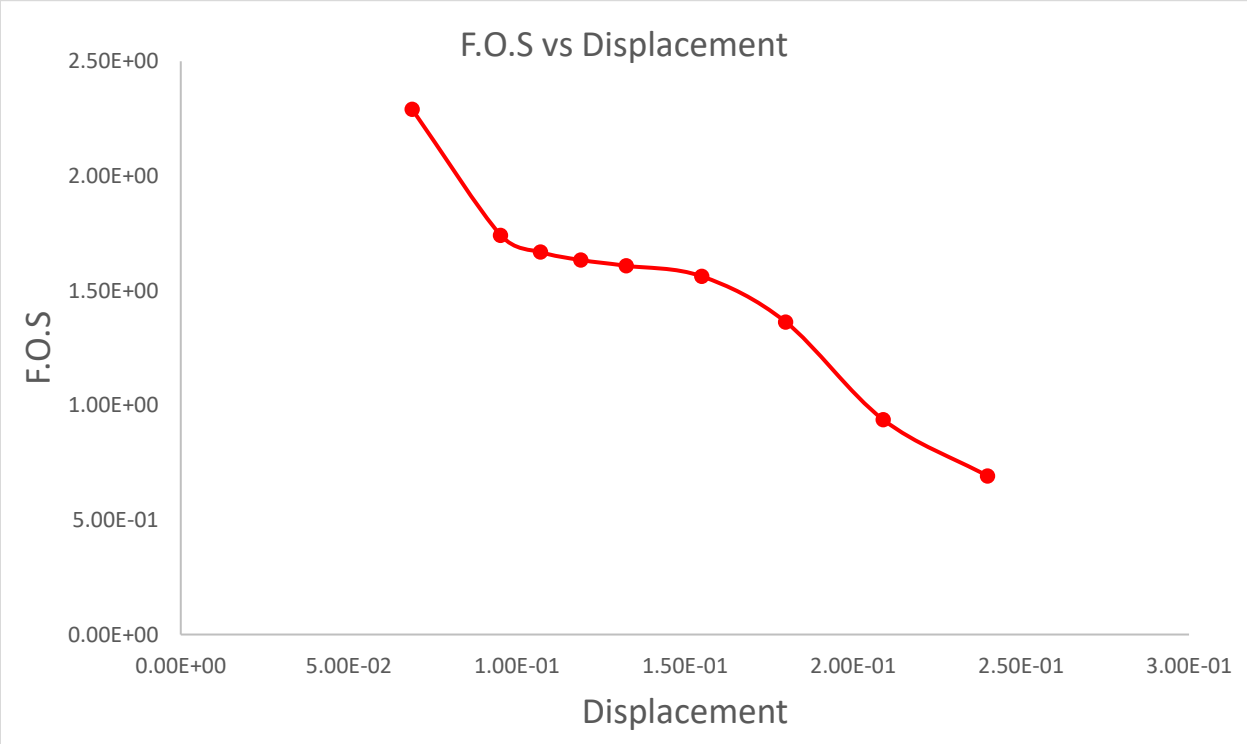

Figure 7-12 – F.O.S vs Displacement - Carbon - Aluminum

7.1.3 Dimension Change

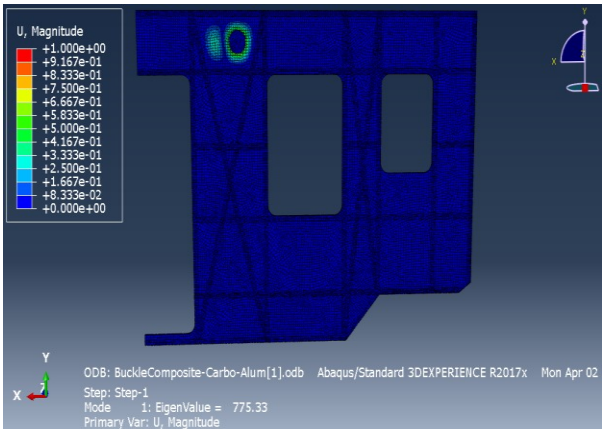

Figure 7-13 Eigenvalue mode 1Carbon-Aluminum

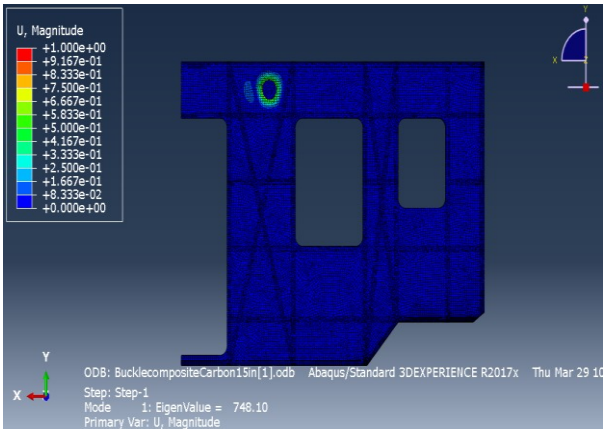

Figure 7-14 Carbon-Nomex

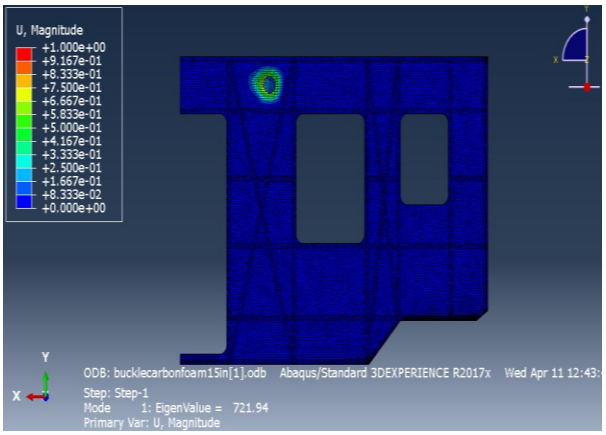

Figure 7-15 Carbon-Foam

7.1.4 Sequence Change

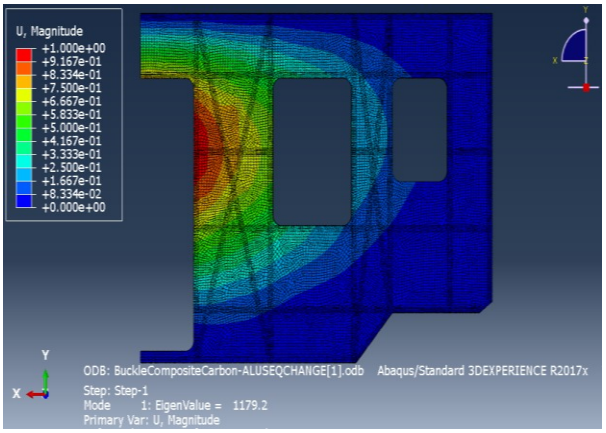

Figure 7-16 E.V. mode 1 Carbon-Aluminum Seq. 1

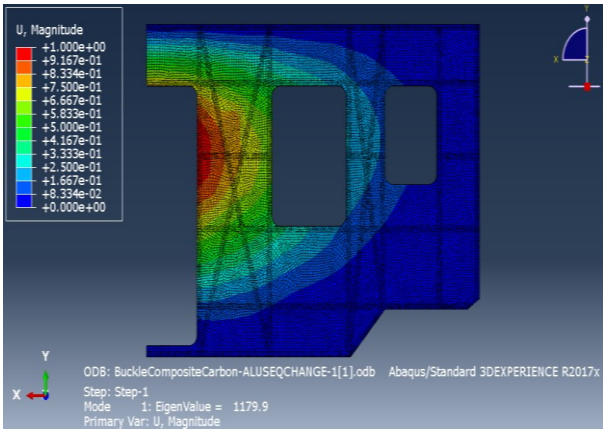

Figure 7-17 Carbon-Aluminum Seq. 2

Material	Carbon-Aluminum	Carbon-Aluminum	Carbon-Nomex	Carbon-Nomex	Carbon-Foam	Carbon-Foam
Thickness	0.2 in	0.15 in	0.2 in	0.15 in	0.2 in	0.15 in
Eigen Value	1170.8	775.33	1089.5	748.10	1072.7	721.94
F.O.S	5.72	3.79	5.32	3.66	5.24	3.53

Table 7-2 Dimension change from 0.2 in to 0.15 eigen value mode 1 and F.O.S Comparison

Material	Carbon-Aluminum	F.O.S		
Eigen Value	1179.2	5.764	Symmetric Layup 1	[90/90/45/90/90/0/90/90/-45]s
Eigen Value	1179.9	5.767	Symmetric Layup 2	[90/90/45/90/90/-45/90/90/0]s

Table 7-3 Sequence change to symmetric layup eigen value mode 1 and F.O.S Comparison

7.1.5 Fasteners Effect on F.O.S

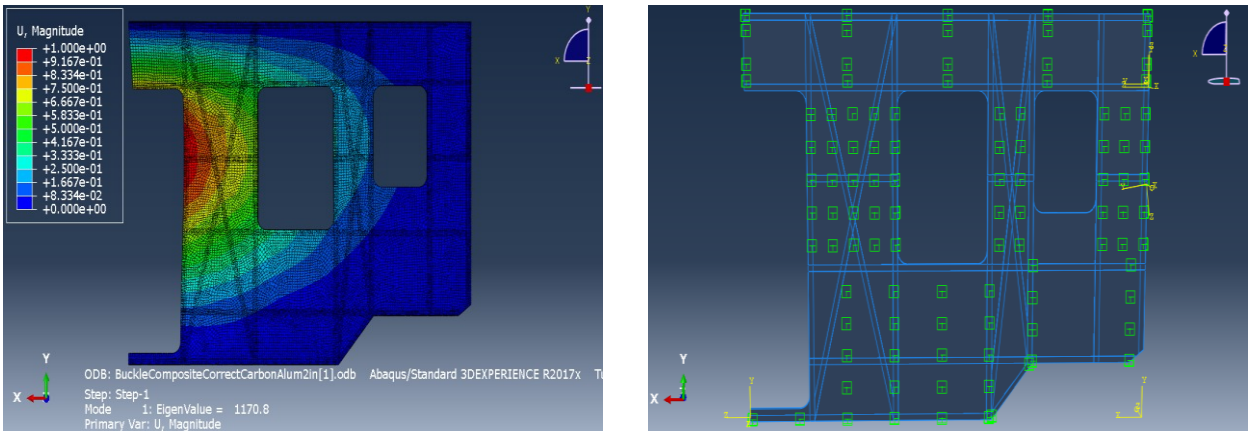

Figure 7-18 Eigenvalue mode 1 Carbon-Aluminum Initial fastener configuration

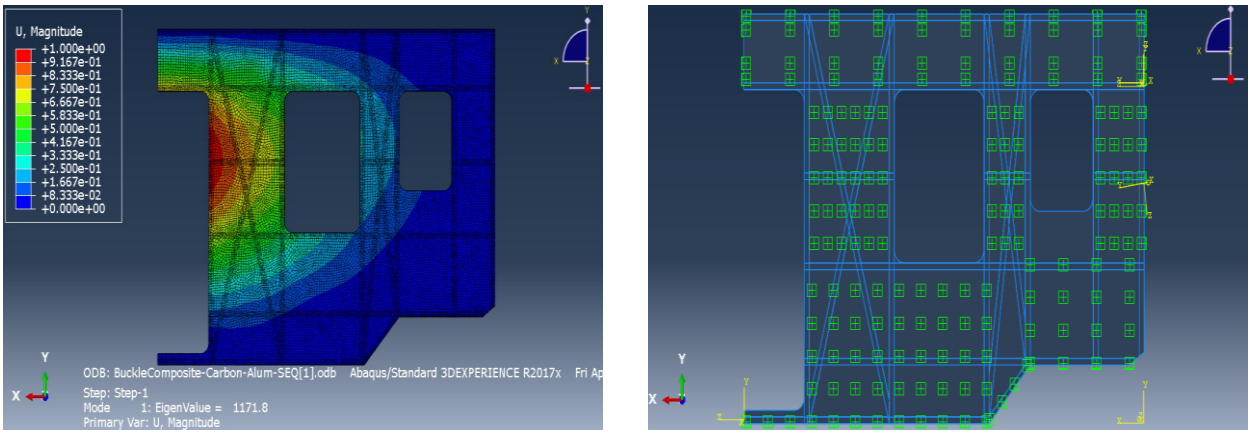

Figure 7-19 Eigenvalue mode 1 Carbon-Aluminum Double fastener configuration

Fasteners Distance	Initial	Double
Eigen Value	1170.8	1171.8
F.O.S	5.723	5.728

Table 7-4 Fasteners spacing change effect on eigenvalue mode 1 and F.O.S Comparison

7.1.6 Mass of Side Wall

Material	Steel	Carbon-Aluminum	Carbon-Nomex	Carbon-Foam	E-Glass-Aluminum	E-Glass-Nomex	E-Glass-Foam
Mass	1879.53	571.61	539.59	519.86	675.59	643.57	623.83

Table 7-5 Mass of side wall Comparison

7.2 Wind Load

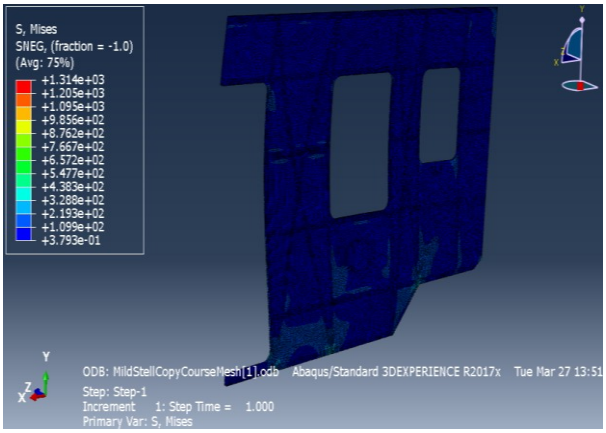

Figure 7-20 Stress Mild Steel

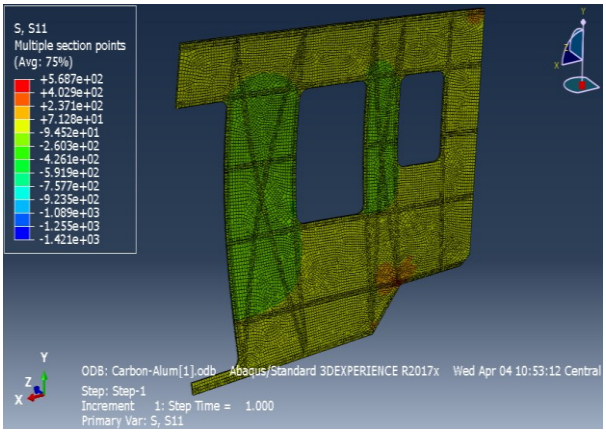

Figure 7-21 Carbon-Aluminum

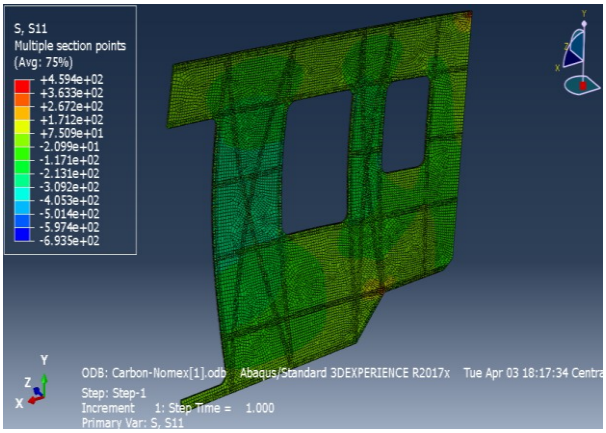

Figure 7-22 Carbon-Nomex

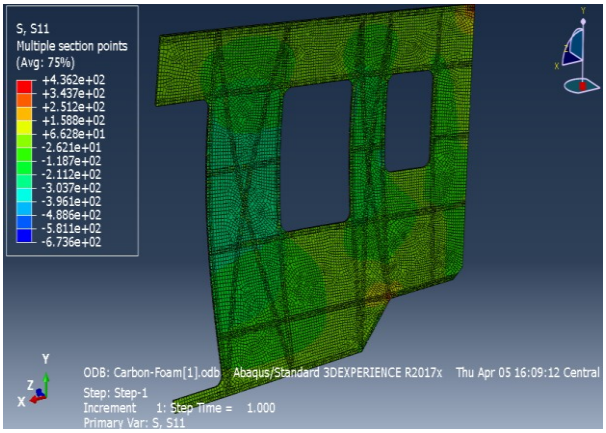

Figure 7-23 Carbon-Foam

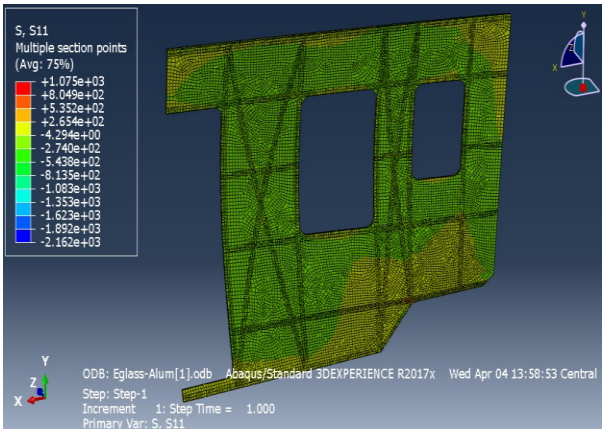

Figure 7-24 E-glass-Aluminum

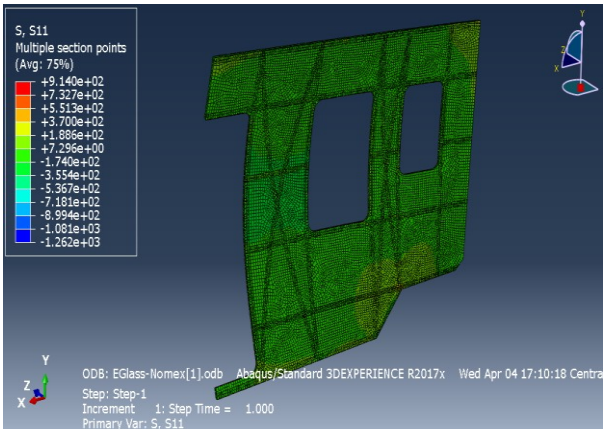

Figure 7-25 E-glass-Nomex

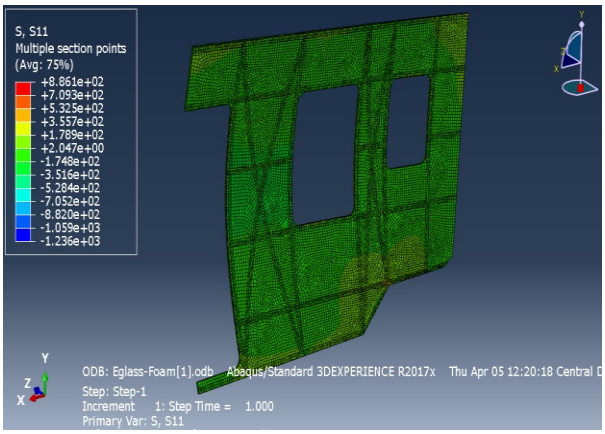

Figure 7-26 E-glass-Foam

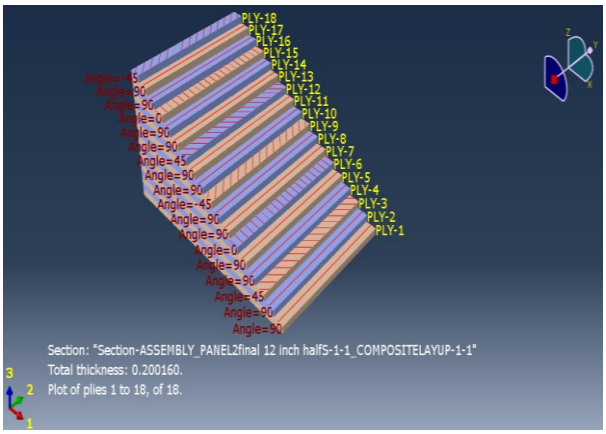

Figure 7-27 Ply Stack – Plot

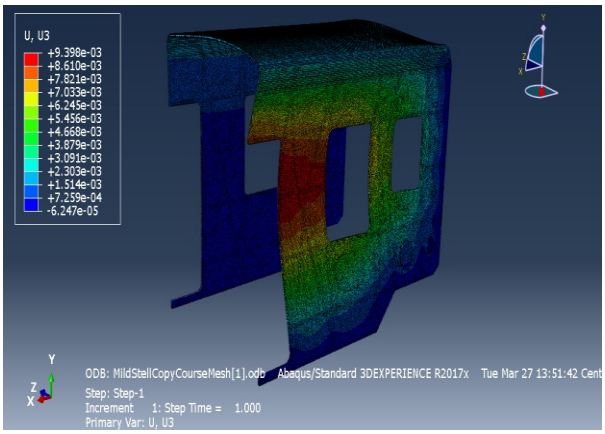

Figure 7-28 Deformation Mild Steel

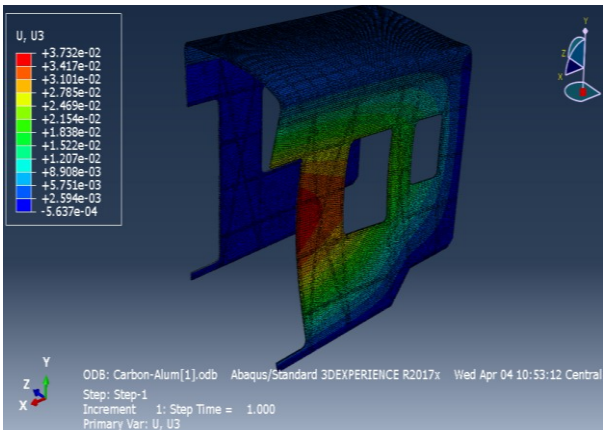

Figure 7-29 Carbon-Aluminum

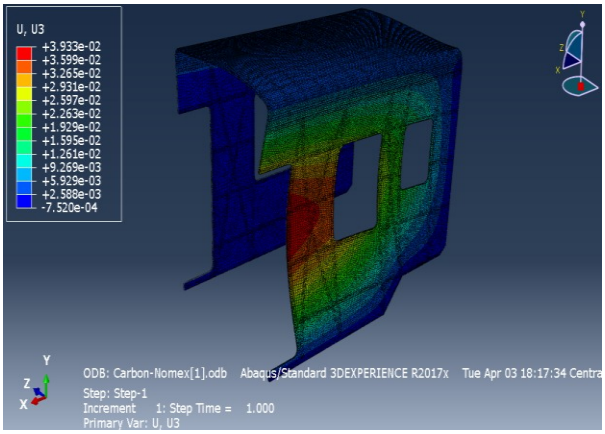

Figure 7-30 Carbon-Nomex

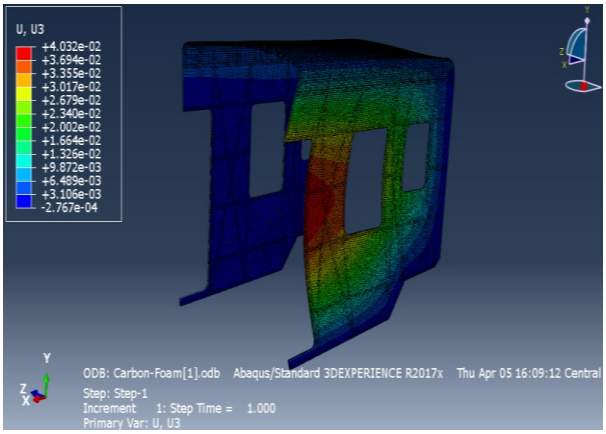

Figure 7-31 Carbon-Foam

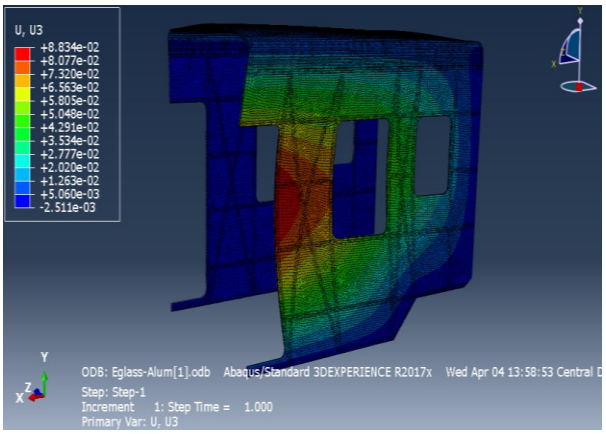

Figure 7-32 E-glass-Aluminum

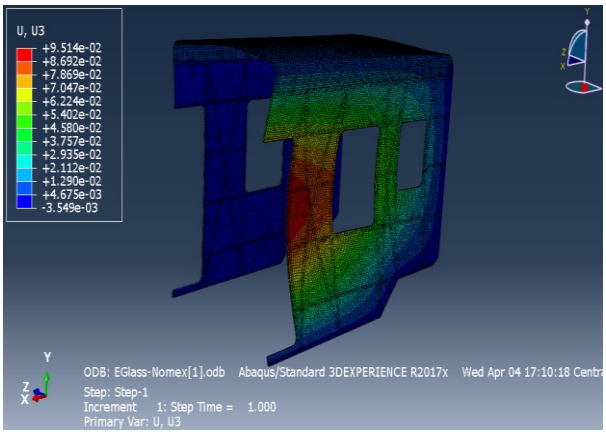

Figure 7-33 E-glass-Nomex

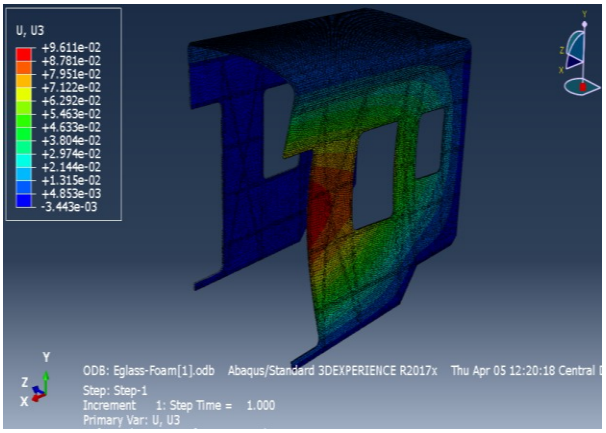

Figure 7-34 E-glass-Foam

7.2.1 Sequence Change

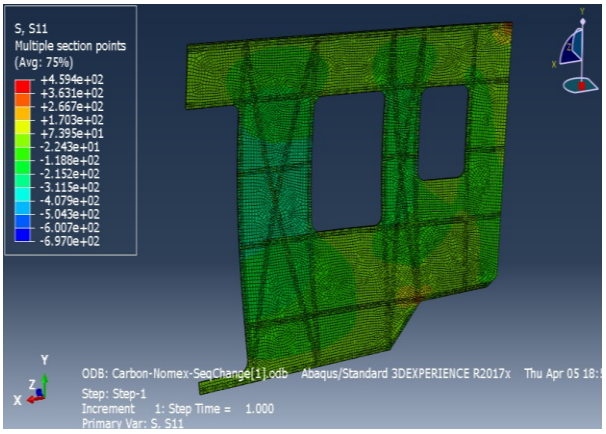

Figure 7-35 Stress Carbon-Nomex Seq. 1

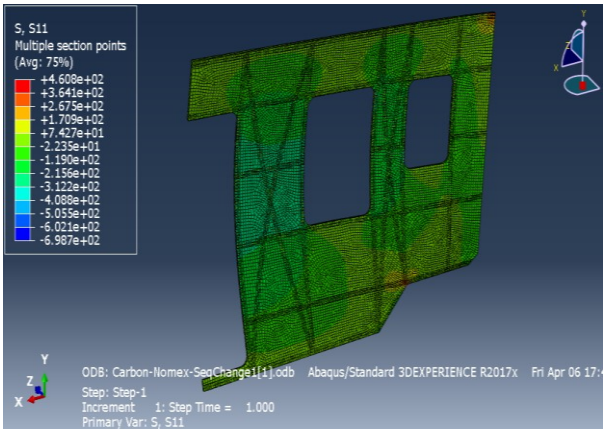

Figure 7-36 Carbon-Nomex Seq. 2

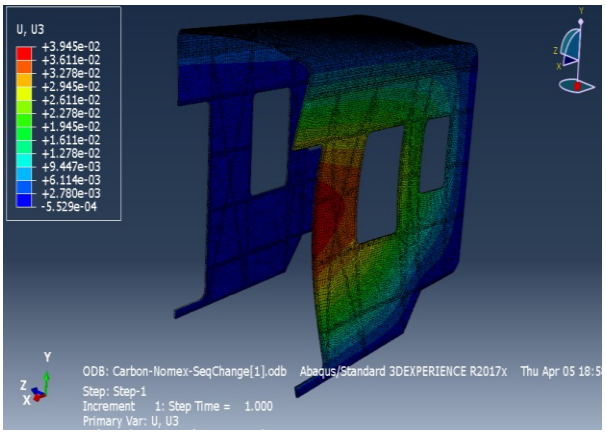

Figure 7-37 Deformation Carbon-Nomex

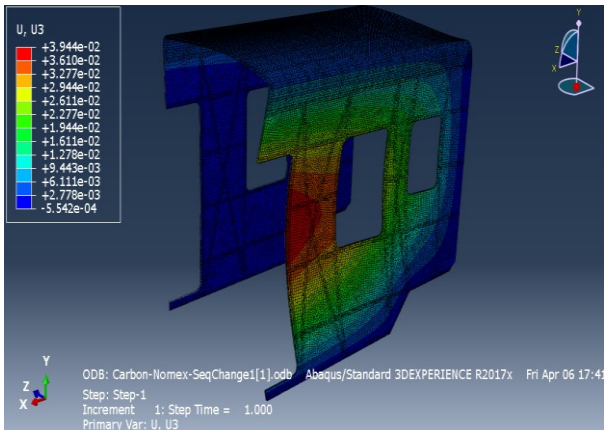

Figure 7-38 Carbon-Nomex

Material	Steel	Carbon-Aluminum	Carbon-Nomex	Carbon Foam	E-glass Aluminum	E-glass Nomex	E-glass Foam
S11	1314 (V.M)	568.7	459.4	436.2	1075	914.0	886.1
S22		5.73	47.51	52.03	131.0	120.0	115.2
S12		105.9	171.0	171.1	166.1	315.5	316.8
Defor-mation in U3	9.3e-03	3.7e-02	3.9e-02	4.0e-02	8.8e-02	9.5e-02	9.6e-02
U2	2.9e-03	1.1e-02	1.1e-02	1.1e-02	2.6e-02	2.8e-02	2.8e-02
U1	1.2e-04	3.1e-04	3.4e-04	3.7e-04	6.9e-04	6.9e-02	7.1e-04
Analytic	9.01e-02	4.1e-01	4.1e-01	4.1e-01	9.9e-01	9.9e-01	9.9e-01
F.O.S	24.34	64.47	79.81	84.05	17.05	20.05	20.69

Table 7-6 Wind load Stress, Deformation, and F.O.S comparison

Material	Carbon-Nomex	Carbon-Nomex Sequence 1	Carbon-Nomex Sequence 2
S11	459.4	459.4	460.8
S22	47.51	47.63	47.55
S12	171.0	171.7	171.7
F.O.S.	79.81	79.81	79.97
Deformation in U3	3.9e-02	3.9e-02	3.9e-02
U2	1.1e-02	1.17e-02	1.13e-02
U1	3.4e-04	3.5e-04	3.5e-04

Table 7-7 Wind load Sequence change to symmetrical layup Stress, Deformation and F.O.S comparison

7.3 Natural Frequency

When the frequency of input load is equal to the frequency of the system, resonance occurs. So, the natural frequency is an important parameter to consider from a design point of view. Units of Frequency is Hz. Same mesh size, fasteners radius, and distance are used as in the case of buckling. Load in the case of Steel is 175,659 lbf, Carbon – Aluminum is 45,160 lbf, E-Glass – Aluminum is 33,742 lbf and approximately same for the other core combinations. [27]

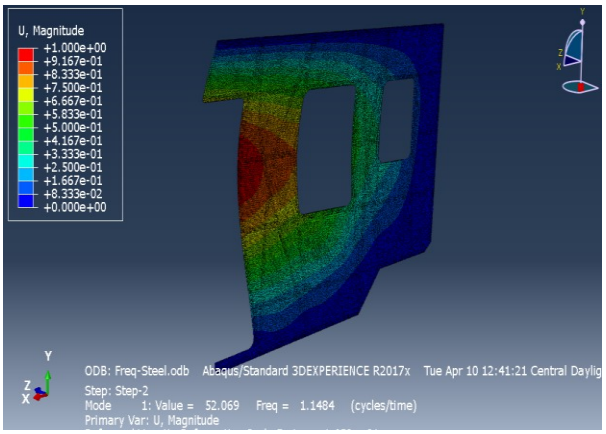

Figure 7-39 Frequency mode 1 Mild Steel

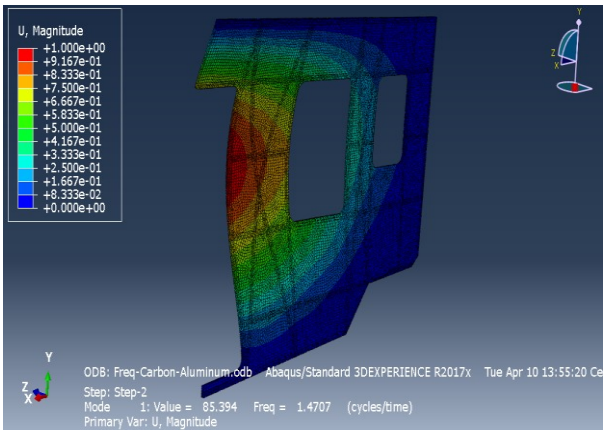

Figure 7-40 Carbon-Aluminum

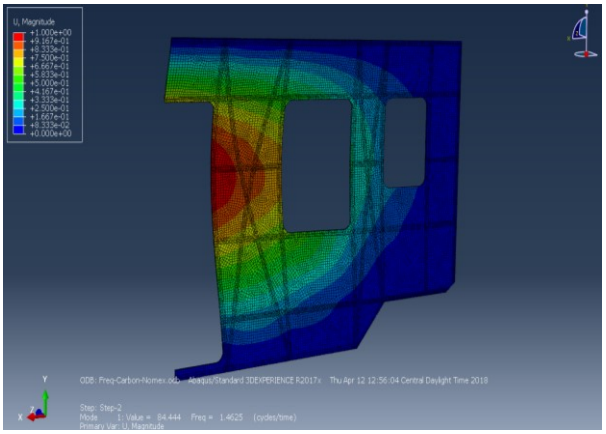

Figure 7-41 Carbon-Nomex

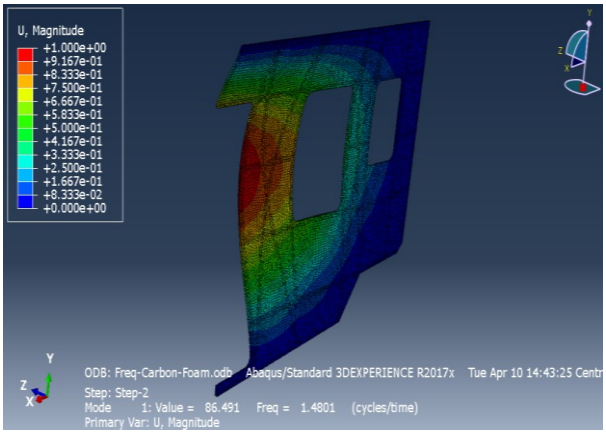

Figure 7-42 Carbon-Foam

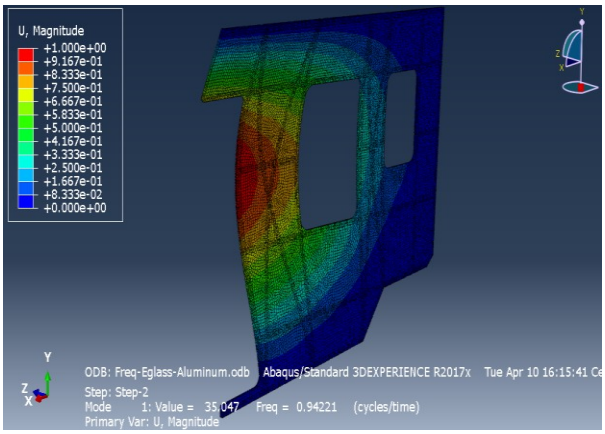

Figure 7-43 E-glass-Aluminum

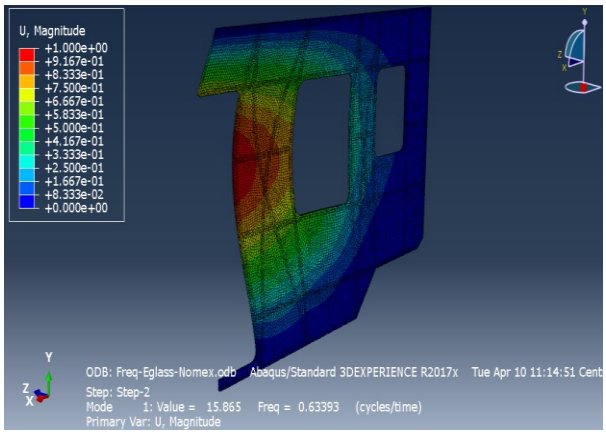

Figure 7-44 E-glass-Nomex

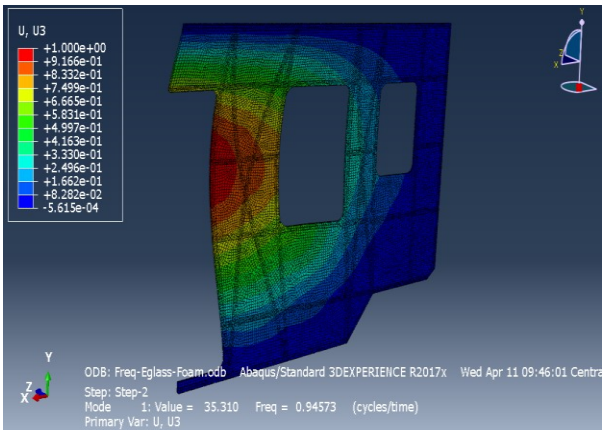

Figure 7-45 E-glass-Foam

7.3.1 Sequence Change

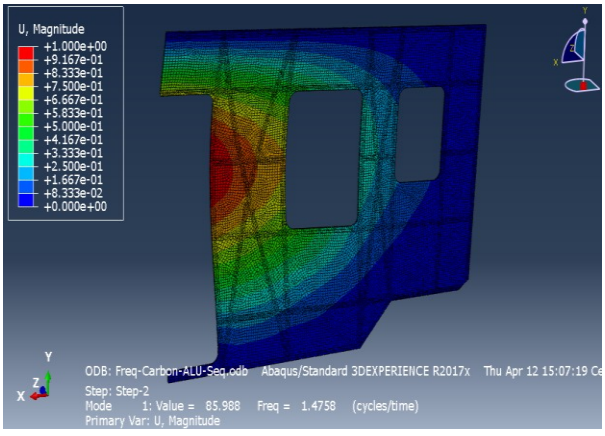

Figure 7-46 Freq. mode 1 Carbon-Aluminum Seq.1

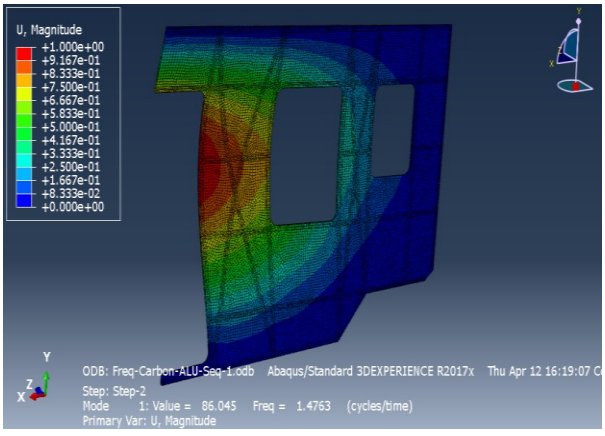

Figure 7-47 Carbon-Aluminum Seq.2

Modes	Steel	Carbon Aluminum	Carbon Nomex	Carbon Foam	E-Glass Aluminum	Carbon Foam	E-Glass Nomex	E-Glass Foam
1	1.14	1.47	1.46	1.48	.95	1.48	0.64	0.95
2	1.88	2.03	1.32	2.03	1.37	2.03	0.96	1.36
3	2.59	2.95	1.82	2.87	1.98	2.87	1.30	1.90
4	3.16	3.75	2.4	3.64	2.4	3.64	1.66	2.34
5	3.20	3.97	2.38	3.80	2.62	3.80	1.70	2.51

Table 7-8 Natural frequency Modes comparison

Modes	Carbon-Aluminum	Carbon-Aluminum Seq1	Carbon-Aluminum Seq2
1	1.4707	1.475	1.476
2	2.03	2.03	2.03
3	2.94	2.93	2.93
4	3.75	3.68	3.65
5	3.95	3.95	3.95

Table 7-9 Natural frequency sequence change to symmetrical layup modes comparison

Chapter 8

Conclusion

1) F.O.S of different Carbon combinations is higher than that of the mild steel in Buckling and Wind load case with the F.O.S of Carbon – Aluminum highest in the 1st case thus increasing the safety.

2) By adding imperfection in Riks analysis, it is concluded that mild steel side wall reaches F.O.S of unity at the vertical displacement of 0.028 in. while using Carbon – Al, side wall reaches F.O.S of unity when vertical displacement is 0.19 in.

3) Composite side walls are lighter, and the Mass reduction is 69.5% in case of Carbon-Aluminum replacing mild steel.

4) The natural frequency of Carbon-Aluminum for Mode 1 is 29% higher than that of steel.

5) Changing the dimensions of the face sheet from 0.2 inches to 0.15 inch cannot consider being safe design even if it has higher F.O.S than mild steel because the load is not distributed evenly, rather it is concentrated in a region above the door.

6) Increasing the number of fasteners doesn't have a significant effect on the increase of F.O.S. so initial configuration of fasteners is acceptable.

7) The experiment shows that 10% reduction in vehicle weight can result in a 6%-8% fuel economy improvement and reducing Co2 emissions. (Wennberg, 2011 #5)

8) The symmetric layup is useful to consider in terms to increase F.O.S.

9) E-glass with different core materials is safe in all the cases but have less F.O.S than that of mild steel in buckling and wind load case.

$$\frac{\text{emissions}}{[\text{g/pass. mile}]} = \frac{\text{EF(g/kWh)} * \text{total electricity consumption [kWh]}}{\left(\text{total passenger miles [pass. miles]} * \text{line loss factor [kWh/kWh]}\right)}$$

Figure 8-1 Emission formula

Chapter 9

Future Work

1. Fasteners can be used in Hexagonal layout and effective distance between the fasteners can be recommended.
2. Different Shape of Stiffeners can be considered to study all the cases.
3. End walls and other interior parts can be made of the composite to reduce the overall weight of railroad car.
4. Core and face sheets thickness can be changed accordingly to increase the space for passengers maintaining the structural integrity.

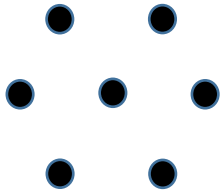

Figure 9-1 Hexagonal layout

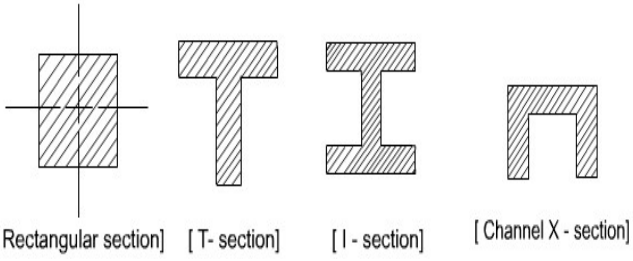

Figure 9-2 Shape of different stiffeners

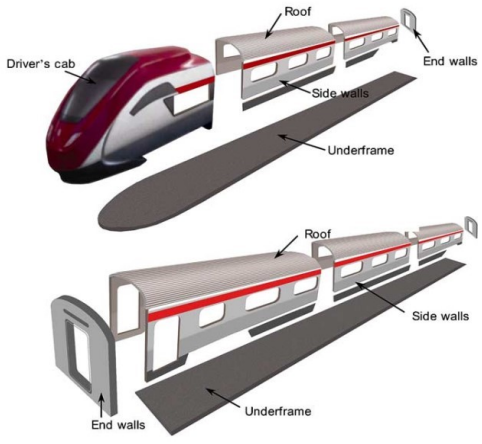

Figure 9-3 Car body

Appendix A

Matlab Code

```
% Script calculates the laminate bending stiffness and calculates the deflection

clear; close all;

% Asymmetric Ply lay-up
%
theta(1)=90; E1(1)=6526698.19; E2(1)=1500000; G12(1)=725188.68; v12(1)=0.3; t(1)=0.0223;
theta(2)=90; E1(2)=6526698.19; E2(2)=1500000; G12(2)=725188.68; v12(2)=0.3; t(2)=0.0223;
theta(3)=45; E1(3)=6526698.19; E2(3)=1500000; G12(3)=725188.68; v12(3)=0.3; t(3)=0.0223;
theta(4)=90; E1(4)=6526698.19; E2(4)=1500000; G12(4)=725188.68; v12(4)=0.3; t(4)=0.0223;
theta(5)=90; E1(5)=6526698.19; E2(5)=1500000; G12(5)=725188.68; v12(5)=0.3; t(5)=0.0223;
theta(6)=0; E1(6)=6526698.19; E2(6)=1500000; G12(6)=725188.68; v12(6)=0.3;   t(6)=0.0223;
theta(7)=90; E1(7)=6526698.19; E2(7)=1500000; G12(7)=725188.68; v12(7)=0.3; t(7)=0.0223;
theta(8)=90; E1(8)=6526698.19; E2(8)=1500000; G12(8)=725188.68; v12(8)=0.3; t(8)=0.0223;
theta(9)=-45; E1(9)=6526698.19; E2(9)=1500000; G12(9)=725188.68; v12(9)=0.3;t(9)=0.0223;
theta(10)=90; E1(10)=6526698.19; E2(10)=1500000; G12(10)=725188.68; v12(10)=0.3;t(10)=0.0223;
theta(11)=90; E1(11)=6526698.19; E2(11)=1500000; G12(11)=725188.68; v12(11)=0.3;t(11)=0.0223;
theta(12)=45; E1(12)=6526698.19; E2(12)=1500000; G12(12)=725188.68; v12(12)=0.3;t(12)=0.0223;
theta(13)=90; E1(13)=6526698.19; E2(13)=1500000; G12(13)=725188.68; v12(13)=0.3;t(13)=0.0223;
theta(14)=90; E1(14)=6526698.19; E2(14)=1500000; G12(14)=725188.68; v12(14)=0.3;t(14)=0.0223;
theta(15)=0; E1(15)=6526698.19; E2(15)=1500000; G12(15)=725188.68; v12(15)=0.3;t(15)=0.0223;
theta(16)=90; E1(16)=6526698.19; E2(16)=1500000; G12(16)=725188.68; v12(16)=0.3;t(16)=0.0223;
theta(17)=90; E1(17)=6526698.19; E2(17)=1500000; G12(17)=725188.68; v12(17)=0.3;t(17)=0.0223;
theta(18)=-45; E1(18)=6526698.19; E2(18)=1500000; G12(18)=725188.68; v12(18)=0.3;t(18)=0.0223;

Qbar=cell(length(theta),1);
%
% Loop through all plies, calculate Qbar for each ply
%
for i=1:length(theta)
v21(i)=v12(i)*(E2(i)/E1(i));
S=[1/E1(i) -v21(i)/E2(i) 0; -v12(i)/E1(i) 1/E2(i) 0; 0 0 1/G12(i)];
c=cosd(theta(i));
s=sind(theta(i));
T=[c^2 s^2 2*c*s; s^2 c^2 -2*c*s; -c*s c*s (c^2 - s^2)];
Sbar=T'*S*T;
Qbar=inv(Sbar);
end
%
% Calulate the z distances for each ply interface
%
```

```
total_thick=sum(t);
z(1)=-total_thick/2;
for k=2:length(theta)+1
z(k)=z(k-1)+t(k-1);
end
%
% Calculate the D matrix
%
D=[0 0 0; 0 0 0; 0 0 0];
for i=1:length(theta)
k=i+1;
Dply=(1/3)*Qbar*(z(k)^3-z(k-1)^3);
D=D+Dply;
end
%
% Applied Transverse Loading
q0=0.032;

%
% Plate dimensions
a=125; b=165;
%

m=[1 3 5 7];
n=[1 3 5 7];
%
% The deflection function expressed in Fourier Expansion
for i=1:length(m)
for j=1:length(n)
den=(D(1,1)*b^4 + 0.571*(D(1,2)+2*D(3,3))*a^2*b^2+ D(2,2)*a^4)

wc=0.00342*q0*a^4*b^4/den;
end
end

% Outputs the Deflection value
wc
% Outputs the Bending Stiffness Matrix to get D16 and D26 values
D
```

*Can be repeated for all other cases

Appendix B

Mesh Convergence

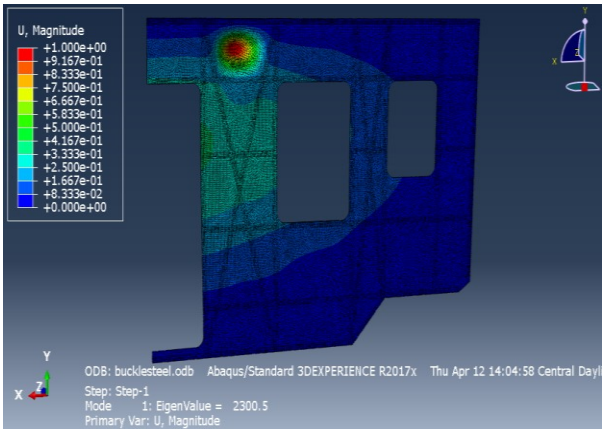

Figure B-1 Mesh size 0.8 inch

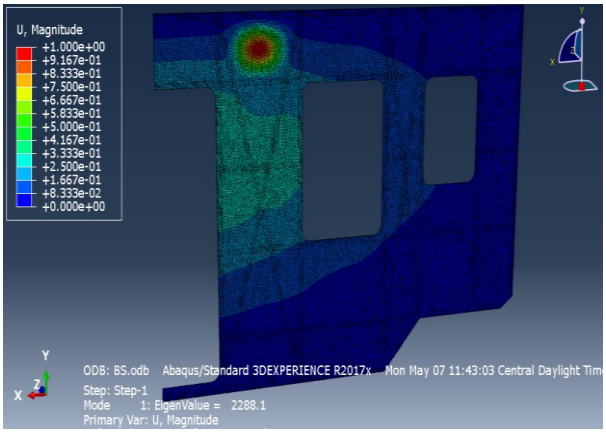

Figure B-2 Mesh size 0.5 inch

In the Figure B-1 which is the case of buckling analysis of carbon steel, mesh size is 0.8 inch and in Figure B-2 mesh size is 0.5 inch which is 37.5% higher mesh density, results in a change of eigenvalue i.e. 0.5%. So, as the change is minimal, I considered 0.8 in. as the optimal mesh size.

References

1. Wennberg, D., *Light-weighting methodology in rail vehicle design through introduction of load carrying sandwich panels*. 2011, KTH Royal Institute of Technology.
2. Wennberg, D., *A light weight car body for high speed trains: Literature study*. 2010: KTH Royal Institute of Technology.
3. Heller, P., J. Korinek, and L. Triska, *Hybrid Body of Underground Railway Car: Path Towards Reduced Weight of Rail Vehicles.* Modern Machinery Science J, 2015: p. 631-634.
4. DART, *Dart SLRV Fact Sheets.*
5. En, B.S., *12663-1: 2010" Railway applications.* Structural requirements of railway vehicle bodies. Locomotives and passenger rolling stock (and alternative method for freight wagons), 2010.
6. Shin, K.B., et al., *Evaluation of the structural integrity of a sandwich composite train roof structure.* WIT Transactions on The Built Environment, 2006. 85 %@ 1845641620.
7. *Honeycomb Panels, Honeycomb Cores*. Available from: www.plascore.com/honeycomb/honeycomb-panels/.
8. Daniel, I.M., et al., *Engineering mechanics of composite materials*. Vol. 3. 1994: Oxford university press New York.
9. Hindawi. *Composite with Fiber and Matrix*. Available from: https://www.hindawi.com/journals/je/2013/450381/fig5/.
10. Kim, J.-S., and S.-K. Chung, *A study on the low-velocity impact response of laminates for composite railway bodyshells.* Composite structures, 2007. 77(4): p. 484-492 %@ 0263-8223.
11. Seo, S.I., J.S. Kim, and S.H. Cho, *Development of a hybrid composite bodyshell for tilting trains.* Proceedings of the Institution of Mechanical Engineers, Part F: Journal of Rail and Rapid Transit, 2008. 222(1): p. 1-13 %@ 0954-4097.
12. Harte, A.M., J.F. McNamara, and I.D. Roddy, *A multilevel approach to the optimisation of a composite light rail vehicle bodyshell.* Composite Structures, 2004. 63(3-4): p. 447-453 %@ 0263-8223.
13. KINKISHARYO, *KinkiSharyo Dallas Area Rapid Transit Technical Data.*

14. Wennberg, D., *Multi-functional composite design concepts for rail vehicle car bodies*. 2013, KTH Royal Institute of Technology.
15. DART, *Dallas Area Rapid Transit (DART) Reference book.*
16. Sepe, R. and A. Pozzi. *Static and modal numerical analyses for the roof structure of a railway freight refrigerated car*. Frattura ed Integritá Strutturale 2015 33]; 451 %@ 1971-8993].
17. Cho, J.G., J.S. Koo, and H.S. Jung, *A lightweight design approach for an EMU carbody using a material selection method and size optimization.* Journal of Mechanical Science and Technology, 2016. 30(2): p. 673-681 %@ 1738-494X.
18. CompositeWorld. *Composite Material*. Available from: https://www.compositesworld.com/articles/composites-101-fibers-and-resins.
19. Jaafar, M., et al., *A 3D FE modeling of machining process of Nomex® honeycomb core: influence of the cell structure behaviour and specific tool geometry.* Procedia CIRP, 2017. 58: p. 505-510 %@ 2212-8271.
20. Hibbitt, Karlsson, and Sorensen, *ABAQUS/Explicit: user's manual*. Vol. 1. 2001: Hibbitt, Karlsson and Sorenson Incorporated.
21. Ties, S.-B. and M.-I.P. Fasteners, *Constraints and Connections.* 2005.
22. Prockat, J., *Developing Large Structural Parts for Railway Application Using a Fibre Reinforced Polymer Design*. Vol. 61 %@ 3798319553. 2005: Univerlagtuberlin.
23. Engineeringtoolbox. *Wind Load Definition Formula*. Available from: https://www.engineeringtoolbox.com/wind-load-d_1775.html.
24. Geoengineering, *Wind Load.*
25. Agarwal, B.D., L.J. Broutman, and K. Chandrashekhara, *Analysis and performance of fiber composites*. 2017: John Wiley & Sons.
26. MIT. *Connector Elements*. Available from: https://abaqus-docs.mit.edu/2017/English/SIMACAEELMRefMap/simaelm-c-connectorelem.htm.
27. Sun, W., et al., *Analysis of modal frequency optimization of railway vehicle car body.* Advances in Mechanical Engineering, 2016. 8(4): p. 1687814016643640 %@ 1687-8140.

Biographical Information

Dilraj Singh, a graduate student in Mechanical engineering at the University of Texas at Arlington, Texas, started his graduate studies in Fall 2016. He did an internship in Dhaliwal Laboratories during summer 2017 as a Mechanical Engineer Intern. He received his bachelor's degree in Aerospace Engineering from the Punjab Technical University in Spring 2016. He also worked as a Junior Design Trainee in Aerosphere during his bachelor's degree. His field of interest is Design and FEA analysis of Railroad/Transportation/Trucking components. He has worked on various projects during his bachelor's degree and published 3 research papers *'Conventional Stress Analysis of Helicopter Skid Landing Gear', 'Divergence Optimization of Nozzle', 'Stress Analysis of Fuselage Section of Passenger Aircraft'* in International Journal of Aerospace and Mechanical Engineering. His knowledge and expertise in the field of design and analysis using FEM, CAD, CAE helped him during this thesis project work. He will keep contributing to the society in the field of Design and FEA analysis.